

AN ABSTRACT OF THE THESIS OF

Soheil Sohrab for the Master of Science  
(Name) (Degree)

Electrical and  
in Electronics Engineering presented on Dec 18 1969  
(Major) (Date)

Title: A METHOD OF CONTROLLING THE LEFT VENTRICULAR  
WALL STRESS OF THE HUMAN HEART

*Redacted for Privacy*  
Abstract approved: John L. Saugen

In this thesis a method is presented for maintaining the left ventricular wall stress of the human heart at a constant level during the systole (active portion of the heart's cycle). This constant stress level makes it possible to take isotonic measurements on the heart muscles.

The left ventricle of the human heart is modeled on a hybrid computer. To accomplish this task certain assumptions as to the shape and muscle characteristics of the left ventricle are made; then the relations for stress and pressure are obtained. The simulating force for this active left ventricle is a curve, simulated by a Diode Function Generator, representing the muscle characteristics of the left ventricle as a function of time. This model substitutes for the portion of an active heart needed to design the control device.

With this model of the left ventricle, a control device is developed, using an analog computer, which acts as a pump controlling the amount of fluid in the left ventricle during the systole. This pump extracts the fluid from the cavity when the stress rises above the desired level and reinjects the fluid into the cavity when the stress falls below this level.

The control device consists of a piston and cylinder assembly with a preloaded spring behind the piston. An electromagnetic feedback control may be used to maintain the stress level. It is not essential, however, since this control system accomplishes the same purpose as a passive device by adjusting the system parameters. The parameter values are given in Chapter III of this thesis. This control device is applicable to any left ventricle within the range of 60 to 150 ml.

Another possible future application of this control device is its use as an auxiliary pump to control the pressure in the left ventricle of a failing human heart. This device could be connected to the aorta. This use of the control device is theoretical and has not yet been tested.

A Method of Controlling the Left  
Ventricular Wall Stress of  
the Human Heart

by

Soheil Sohrab

A THESIS

submitted to

Oregon State University

in partial fulfillment of  
the requirements for the  
degree of

Master of Science

June 1970

APPROVED:

*Redacted for Privacy*

Associate Professor of Electrical and Electronics  
Engineering

in charge of major

*Redacted for Privacy*

Head of Department of Electrical and Electronics  
Engineering

*Redacted for Privacy*

Dean of Graduate School

Date thesis is presented Dec. 18, 1969

Typed by Barbara Eby for Soheil Sohrab

## ACKNOWLEDGEMENT

I would like to thank Dr. John Saugen for his recommendations and help in getting me started on this very interesting and challenging project, and also for the informative course taught by him on the programming of hybrid computers.

My thanks to the Department of Electrical Engineering for the use of the hybrid computer EAI 690 in the course of my experiments.

I would like to give my sincere thanks and appreciation to Mrs. Barbara Hadley for her concern, encouragement and help in correcting and typing of the thesis and for proof-reading of the final copy.

Also my thanks and appreciation to Miss Jacqueline Bescup for primary correction of the English.

## TABLE OF CONTENTS

I.	INTRODUCTION	1
	Introduction	1
	Statement of the Problem	2
	Method of Modeling the Left Ventricle	2
	Control Devices	6
	Results and Discussion	9
	Control Device I	10
	Control Device II	15
	A Consideration of the Operation of the Control Device if Used as an Auxiliary Pump to the Left Ventricle of the Heart	18
	Literature Review	21
	Recommendations	23
II.	MODEL OF THE LEFT VENTRICLE OF THE HUMAN HEART	26
	Shape of the Left Ventricle	27
	Muscle Surrounding the Left Ventricular Cavity	28
	Muscle Contractance Curve	28
	Derivation of Formulae Leading to Pressure Calculation	29
	a. Volume of Fluid in the Left Ventricular Cavity	29
	b. Internal and External Radii of the Left Ventricle	30
	c. Wall Stress	31
	d. Pressure	33
III.	CONTROL DEVICES	34
	Control Device I	34
	Magnitude Scaling	37
	Time Scaling	37
	Parameter Values	39
	Control Device II	40
	Magnitude Scaling	43
	Time Scaling	44
	Parameter Values	45
	BIBLIOGRAPHY	47

APPENDIX A	
Generation of the Muscle Contractance Curve by a Diode Function Generator	50
APPENDIX B	
Analog and Digital Computer Diagrams	53
APPENDIX C	
Experimental Results from the EAI 8875 Strip- Chart Recorder	60
APPENDIX D	
Personal Communication (7)	68

## LIST OF FIGURES

<u>Figure</u>		<u>Page</u>
1.1	Schematic diagram of the control set-up for isotonic measurements in open heart surgery.	3
1.2	Block diagram of the control method for controlling the stress level in the left ventricle.	7
1.3	Schematic diagram of the control mechanisms.	8
1.4	Block diagram of the approximated model of the left ventricle with controlled stress level, using the control device I., on a hybrid computer.	11
1.5	Stress level versus preloading.	14
1.6	Block diagram of the approximated model of the left ventricle with controlled stress level, using the control device II., on a hybrid computer.	16
1.7	Schematic diagram of the possible use of the control device I as an auxiliary pump to control the left ventricular pressure.	19
1.8	Rate of flow versus time for the uncontrolled and controlled left ventricle.	20
1.9	Cross-section of the assumed right and left ventricular configuration.	22
1.10	Arterio-arterial pumps.	24
2.1	Cross-section of the left ventricular cavity.	31
2.2	Stress profile in the muscle cross-section.	31
3.1	Free-body diagram of $m$ .	35
3.2	Free-body diagram of $m_1$ .	40
3.3	Free-body diagram of $m_2$ .	41



<u>Figure</u>		<u>Page</u>
A. 1	Muscle contractance curve, $\delta$ .	50
A. 2	Analog computer diagram of a triangular wave generator.	51
A. 3	Block diagram for the generation of muscle contractance curve, $\delta$ .	51
B. 1	Analog computer diagram of the first control system with interface shown.	54
B. 2	Analog computer diagram of the second control system with interface shown.	56
B. 3	Flow diagram for the digital computer portion of the system.	58
C. 1	The effect of preloading of the spring $F_s(0)$ in the control device I, without any other changes, on controlling of the stress level, (a) $F_s(0) = 0$ , (b) $F_s(0) = .015$ , (c) $F_s(0) = .02$ , (d) $F_s(0) = .025$ .	61
C. 2	The influence of the magnetic force, $F_m$ , on control of the stress level in the left ventricle. (a) $F_m = .008$ , (b) $F_m = .03$ .	62
C. 3	Comparison of the stress profiles in the left ventricle when (a) uncontrolled (b) controlled without electromagnet (c) controlled with electromagnet, using control device I when volume, $V_T$ is 60 ml.	63
C. 4	Comparison of the stress profiles in the left ventricle when (a) uncontrolled (b) controlled without electromagnet (c) controlled with electromagnet, using control device I when volume, $V_T$ , is 100 ml.	64
C. 5	Comparison of the stress profiles in the left ventricle when (a) uncontrolled (b) controlled without electromagnet (c) controlled with electromagnet using control device I when volume, $V_T$ , is 150 ml.	65

<u>Figure</u>		<u>Page</u>
C. 6	The delayed effect of the feedback electromagnetic control in the control device II.	66
C. 7	Comparison of the stress profiles in the left ventricle when (a) uncontrolled (b) controlled without electromagnet (c) controlled with electromagnet using control device II.	67

## LIST OF TABLES

<u>Table</u>		<u>Page</u>
A. 1	DFG settings for the generation of $\delta$ .	52
B. 1	Pot settings corresponding to the Figure B. 1 for the analog simulation of the control device I.	55
B. 2	Pot settings corresponding to the Figure B. 2 for the analog simulation of the control device II.	57
B. 3	Digital computer program using Fortran IV language.	59

## NOMENCLATURE

<u>Symbol</u>	<u>Definition</u>	<u>Units</u>
$A_I$	Internal area of the left ventricular cavity	$\text{cm}^2$
$A_P$	Area of the plunger (cross section)	$\text{cm}^2$
$A_T$	Area of the inner surface of the left ventricle when at rest and completely filled	$\text{cm}^2$
CF	Coefficient of frequency	
DV	Volume of fluid displaced, $(V_T - V_L)$	$\text{cm}^3$
$e_x$	Normalized variable defined by Equation (3.11)	per unit
$e_{x_1}$	Normalized variable defined by Equation (3.27)	per unit
$e_{x_2}$	Normalized variable defined by Equation (3.27)	per unit
$e_f$	Normalized variable defined by Equations (3.11), (3.27)	per unit
$e_{f_s}(0)$	Normalized variable defined by Equations (3.11), (3.27)	per unit
$F_f$	Friction force	dynes
$F_I$	Inertial force	dynes
$F_m$	Electromagnetic force	dynes
$F_p$	Pressure force on the plunger	dynes
$F_s$	Spring force	dynes
$F_s(0)$	Constant preloading force of the spring	dynes
$k_f$	Coefficient of friction	

<u>Symbol</u>	<u>Definition</u>	<u>Units</u>
$k_s$	Coefficient of spring	dynes/cm
$k_{s_1}$	Coefficient of the spring in the back of the first plunger	dynes/cm
$k_{s_2}$	Coefficient of the spring in the back of the second plunger	dynes/cm
$k_v$	Coefficient of viscous damping	dynes/cm/sec
$k_{v_1}$	Coefficient of viscous damping for the first plunger	dynes/cm/sec
$k_{v_2}$	Coefficient of viscous damping for the second plunger	dynes/cm/sec
$m$	Mass of the plunger in the first control system	grams
$m_1$	Mass of the first plunger in the second control system	grams
$m_2$	Mass of the second plunger in the second control system	grams
$P$	Pressure in the left ventricle	dynes/cm <sup>2</sup>
$R_I$	Inner radius of the left ventricle	cm
$R_O$	Outer radius of the left ventricle	cm
$s$	Stress on the walls of the left ventricle	dynes/cm <sup>2</sup>
$s_{ref}$	Reference stress	dynes/cm <sup>2</sup>
$S$	Laplace operator	
$t$	Real time	sec
$T$	Computer time	sec
$V_L$	Volume of fluid left in the left ventricular cavity	cm <sup>3</sup>

<u>Symbol</u>	<u>Definition</u>	<u>Units</u>
$V_M$	Muscle volume	$\text{cm}^3$
$V_T$	Inner volume of the left ventricle when at rest and completely filled	$\text{cm}^3$
$x$	Position of the plunger in the first control system	cm
$x_1$	Position of the first plunger in the second control system	cm
$x_2$	Position of the second plunger in the second control system	cm
$\delta$	Muscle contractance curve of the left ventricle	per unit
$\eta$	Time scaling factor	

# A METHOD OF CONTROLLING THE LEFT VENTRICULAR WALL STRESS OF THE HUMAN HEART

## I. INTRODUCTION

### Introduction

Theories have been developed to explain muscular contraction and the structure of the contractile elements in the muscles (20). Much work has been done to acquire more accurate knowledge of the mechanochemical properties of active muscles. A current topic of heart research is the investigation of the heart muscle structure and its mechanochemical properties. This investigation needs to be done on an active heart and requires special control, recording, and measuring devices (2). These structural and chemical studies should help to understand and perhaps control heart actions (20).

Studies concerning the contraction of heart muscle fibers require structural data obtained from isometric and isotonic measurements on the heart muscles during normal operating conditions. Isometric measurements are executed holding the length of the heart muscles constant (6). Isotonic measurements are carried out while the stress on the heart muscles is kept constant (7, Appendix D). Research has been done on isometric measurements and some data has been obtained using dogs and rats (2, 3, 5, 6). However, isotonic

measurements have not been carried out due to the lack of an appropriate control device to keep the stress in the left ventricle at a constant level during the contraction of the left ventricle.

In this thesis two control methods are developed to achieve the constant stress level in the left ventricle necessary for isotonic measurements. First, an approximate model of the left ventricle of the human heart is modeled on a hybrid computer. Then two control methods are tested using the hybrid computer model of the left ventricle.

### Statement of the Problem

Measurements obtained from an active heart when the stress is kept at a constant level are called isotonic measurements. When isotonic measurements are made, the stress on the walls of the left ventricle of the human heart must be maintained constant during the contraction of the left ventricle. To obtain these measurements a control device is needed which can be connected to the left ventricle to compensate for the stress changes manifest in the heart (Figure 1.1).

### Method of Modeling the Left Ventricle

In modeling the left ventricle the shape of the cavity plays an important role in the study of the cardiac properties. Two factors



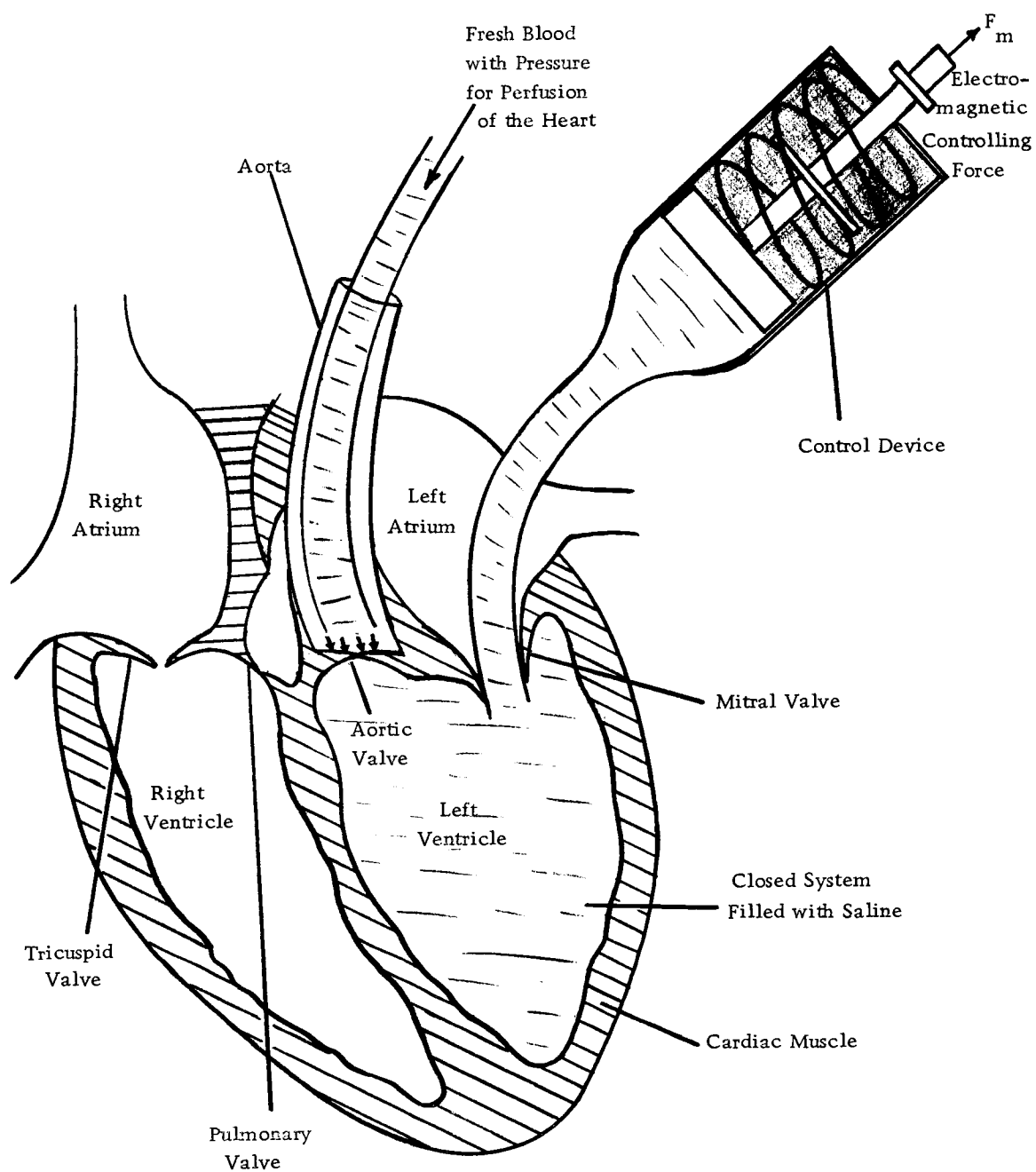


Figure 1.1. Schematic diagram of the control set-up for isotonic measurements in open heart surgery.

are to be considered in choosing an appropriate shape for the left ventricle. The model must have the characteristics of the left ventricle in a similar situation, and this shape must be mathematically presentable. After an extensive study, J. E. W. Beneken suggests that the left ventricle can be approximated by a spherical shell with uniform thickness. He further adds that "the more complicated configurations make calculations extremely difficult" (1, page 88). In this thesis, Beneken's suggestion is assumed to be a good approximation for the shape of the left ventricle.

In modeling the left ventricle further assumptions must be made:

1. The operation of the left ventricle is independent of the rest of the heart, as far as the heart muscle is concerned (1, page 88).
2. The volume of the muscle surrounding the left ventricular cavity is assumed constant during the expansion and contraction of the left ventricle.(1, page 110).
3. The control device is connected to the mitral valve (a small hole in the spherical shell), the aortic valves are closed, and the system filled with fluid to form a closed system. Dr. Covell describes this approach as follows:

"In this preparation the heart is removed from the chest and perfused by a cannula in the aorta so that the aortic valves are closed. A cannula is then inserted in

the mitral valve and the left ventricle filled with saline. . . . A bellofram or plunger and barrel arrangement will be used to form a closed fluid (saline) filled system" (7, Appendix D).

The control device is basically a plunger assembly connected to the left ventricle, as suggested by Covell. When the device is joined to the left ventricle, the position of the piston decides the volume of fluid displaced and therefore the volume of fluid left inside the cavity. Given the muscle volume and the muscle contractance curve, stress and pressure inside the left ventricle may be calculated at any time, using the following formulae. These formulae are derived in Chapter II of this thesis.

$$V_L = V_T - DV \quad (1.1)$$

$$s = \delta \left( \frac{V_L}{V_T} \right)^{2/3} \quad (1.2)$$

$$P = s \left[ 1 - \left( \frac{V_L}{V_M + V_L} \right)^{2/3} \right] \quad (1.3)$$

where

DV = the volume of fluid displaced,

$V_L$  = the volume of fluid left in the left ventricular cavity,

$V_T$  = the total volume of fluid in the cavity,

s = the stress on the walls of the left ventricle,

$\delta$  = the muscle contractance,

P = the pressure inside the left ventricle, and

$V_M$  = the muscle volume.

### Control Devices

Two control devices have been developed, both of which act as pumps pulling the fluid out of the left ventricular cavity whenever the stress rises above a certain desired level and forcing the fluid back into the cavity when the stress falls below the desired level (Figure 1.3). In this process the calculated stress level is compared to the desired stress level and the position of the plunger is accordingly adjusted. The block diagram of this control method is shown below in Figure 1.2.

In order to simulate the control devices the differential equations of the mechanical systems were modeled on an analog computer. The general differential equations of the first and second methods are written below:

For Control Device I the equation is:

$$\ddot{x} = -\frac{k_v}{m} \dot{x} - \frac{k_s}{m} x + \frac{A_p}{m} P + \frac{F_m}{m} - \frac{F_s(0)}{m} \quad (1.4)$$

where

$x$  = position of the plunger,

$m$  = mass of the mechanical system,

$k_v$  = coefficient of viscous damping,

$k_s$  = spring constant,

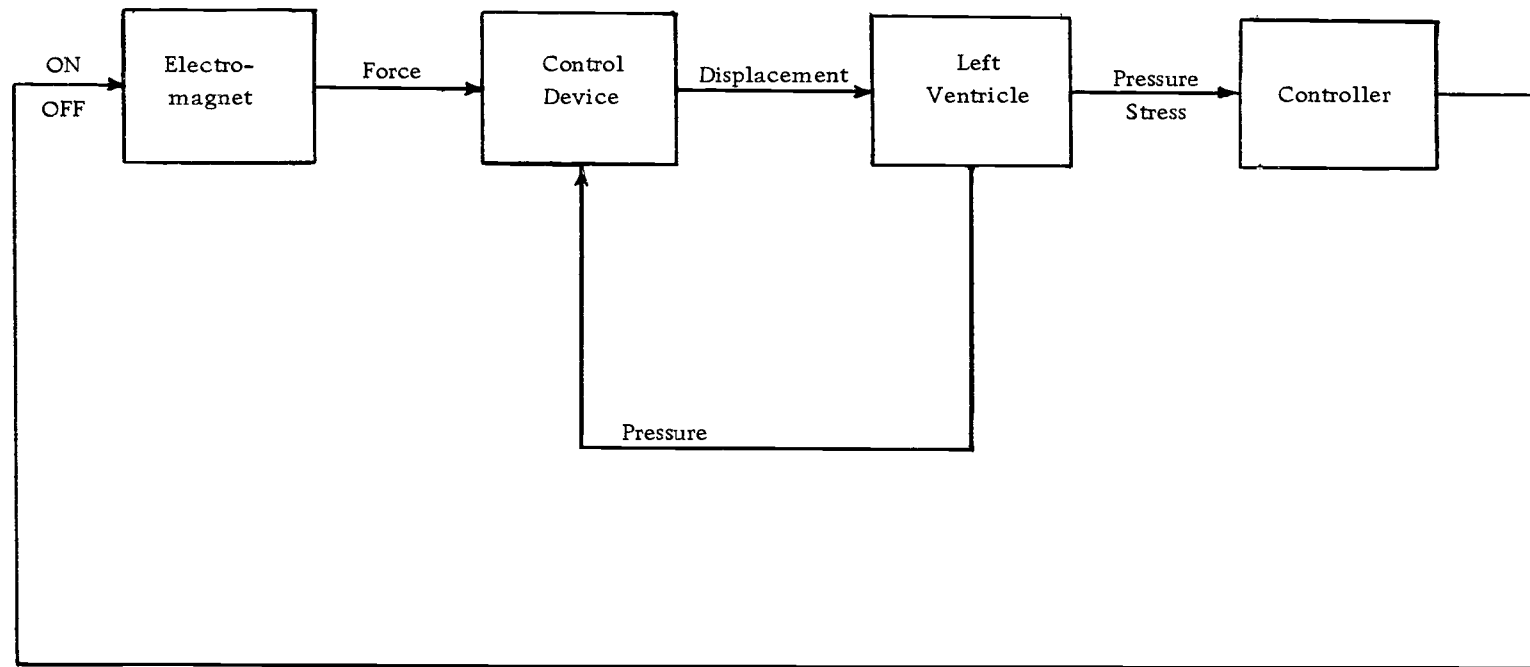
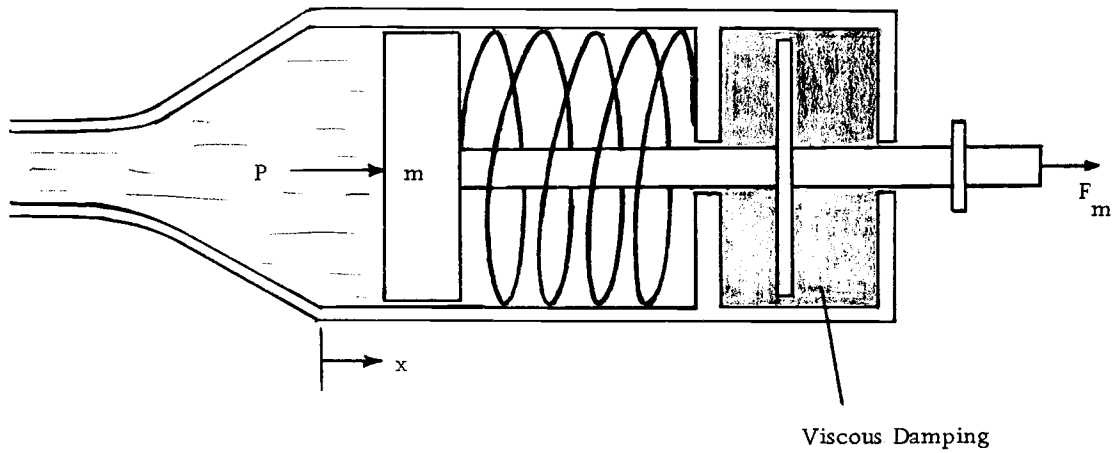
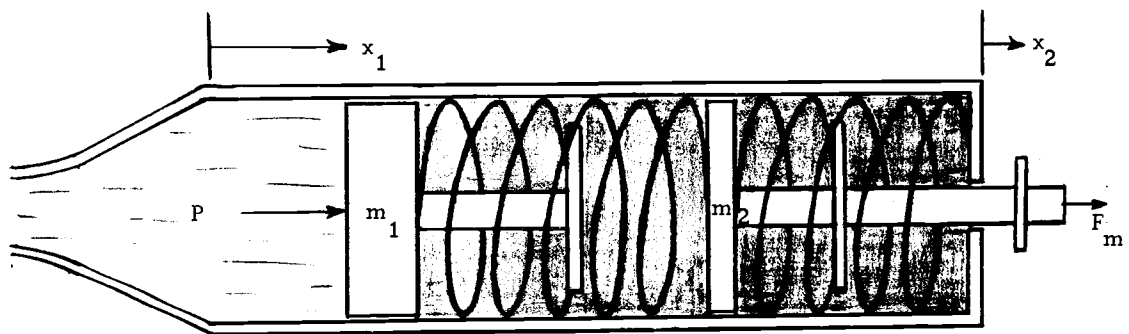


Figure 1.2. Block diagram of the control method for controlling the stress level in the left ventricle.



(a) Control Device I



(b) Control Device II

Figure 1.3. Schematic diagram of the control mechanisms.

$A_p$  = area of the plunger,

$P$  = pressure measured by the transducer,

$F_m$  = electromagnetic force, and

$F_s(0)$  = constant preloading force of the spring.

For Control Device II the equations are:

$$\ddot{x}_1 = -\frac{k_{v1}}{m_1} \dot{x}_1 - \frac{k_{s1}}{m_1} (x_1 - x_2) + \frac{A_p}{m_1} P \quad (1.5)$$

$$\ddot{x}_2 = -\frac{k_{v2}}{m_2} \dot{x}_2 - \left(\frac{k_{s1}}{m_2} + \frac{k_{s2}}{m_2}\right) x_2 + \frac{k_{s1}}{m_2} x_1 + \frac{F_m - F_s(0)}{m_2} \quad (1.6)$$

where

the nomenclature used is the same as in the Equation (1.4), except that the subscripts indicate to which plunger the terms refer, i. e., 1 refers to the first piston and spring, and 2 refers to the second piston and spring (Figure 1.3(b)). The Equations (1.4), (1.5) and (1.6) are developed in Chapter III.

### Results and Discussion

A control system capable of holding the isotonic state in the left ventricle of the heart was achieved. This control system is in the form of a piston and cylinder as described on page 5. All the results were obtained using a hybrid-computer model of the left

ventricle in conjunction with the analog computer simulation of the control devices.

Two different control devices have been developed and tested using the modeled left ventricle. Both devices keep the stress within  $\pm 3\%$  of a given level (Appendix C).

### Control Device I

The first system which maintains the isotonic state in the left ventricle consists of a viscously damped plunger composed of a single mass and spring (Figure 1.3(a)). The detailed block diagram of this system is shown in Figure 1.4. The characteristics and results of this control device are discussed below.

1. An electromagnet is used to pull the plunger out and a spring to push it back in, according to action specified by feedback control.
2. This control device holds the isotonic state in the left ventricle both as an active and a passive device; i. e., it will keep the stress level constant even if the electro-magnetic control is disconnected (Figure C.3). The stress profile when the feedback control is applied changes very slightly from the stress profile of the system without feedback control. In the case of the active system the stress profile is very sharply cut at the desired level and this



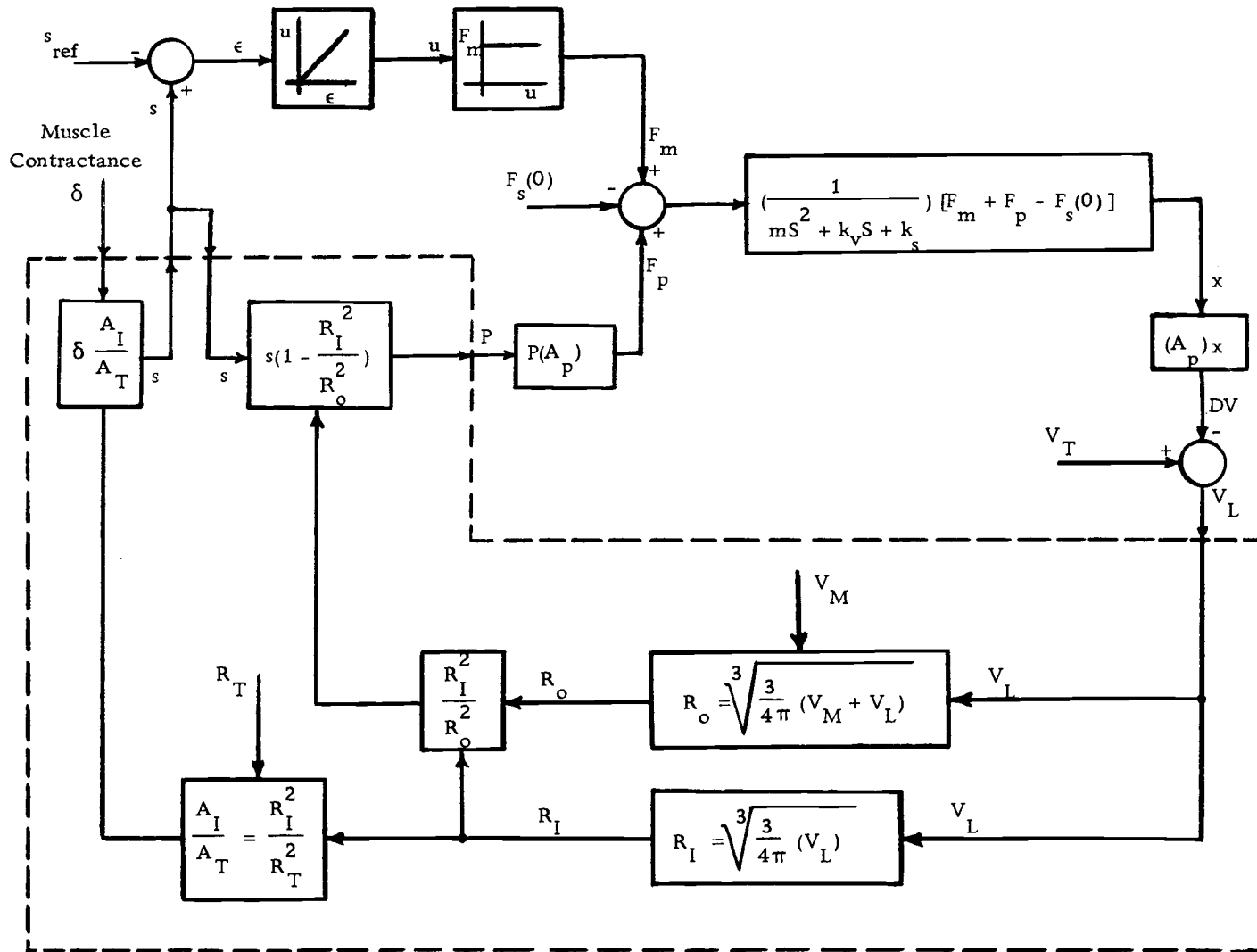


Figure 1.4. Block diagram of the approximated model of the left ventricle with controlled stress level, using the control device I, on a hybrid computer. (The portion enclosed within the broken line is simulated on the digital computer and the rest on the analog computer.)

constant level is maintained longer. In the case of the passive system the stress changes are gradual. Thus the corners are rounded and the duration of constant stress level is slightly shorter.

3. This simulated device was tested on three different sizes of the left ventricle, at volumes of 60 ml., 100 ml., and 150 ml. The results of these experiments for the three volumes are shown in Figures C.3, C.4, and C.5.

Figures corresponding to each different volume of the left ventricle show the comparison of the stress profiles for the following three conditions:

- a. No control device is connected to the left ventricle.

The stress profile in this case shows the maximum stress reached in the left ventricle without external help.

- b. The passive device, i. e., the piston and cylinder assembly without any feedback or electromagnetic control is connected to the left ventricle. The passive device maintained the constant stress level for all three sizes, without any change in the device. The stress level can be adjusted by changing the preloading on the spring--using a larger preloading for a higher stress level.

- c. The control device is connected to the left ventricle and fully used; i. e. , feedback control is applied and an on-off electromagnet is energized to control the position of the piston. In this case, to maintain the constant stress level, the reference stress level and the force of the electromagnet were adjusted for different volumes:

<u>Volume</u>	<u>Reference Stress</u>	<u>Force of Electromagnet</u>
60 ml.	. 5	. 01
100 ml.	. 57	. 01
150 ml.	. 65	. 015

This control device is effective within a volume range of 60 to 150 ml. This range can be increased by greater adjustments of the preloading and the electromagnetic force. Examination of volumes larger and smaller than those above was not deemed necessary, since the left ventricular volume of a human heart does not vary more than 60 to 150 ml.

4. The spring in the device was preloaded, so that the pressure had to reach a certain level, decided by the amount of this preloading, before the plunger began to move. On the passive device (no control force), many tests were

performed for different magnitudes of preloading on the spring and the resulting stress level was recorded. These data are plotted in Figure 1.5 below as stress level versus preloading of the spring.

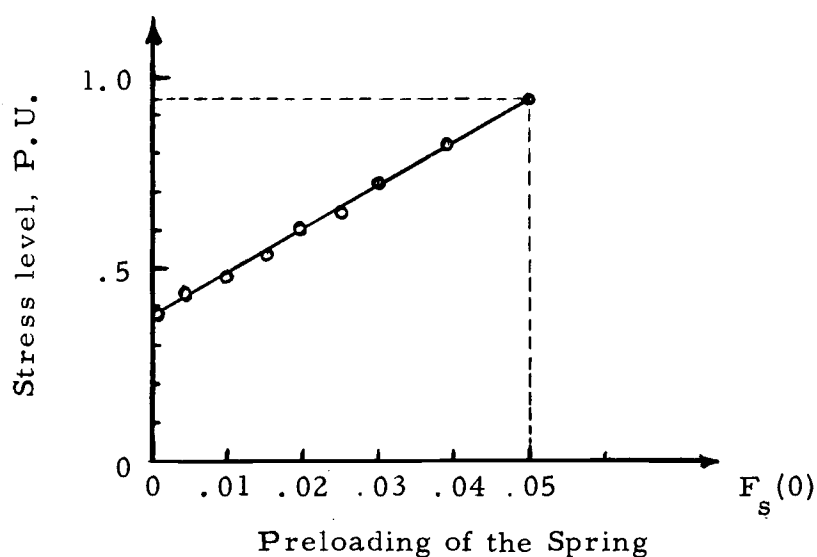


Figure 1.5. Stress level versus preloading.

This shows that the stress level can be controlled, within certain limits, by merely adjusting the preloading and without any use of feedback control (Figure C.1). However, one should also note that the period of constant stress varies inversely with the stress level; that is, the higher the stress level, the shorter the duration of constant stress level during which measurements can be made.

5. The stress level may also be controlled using the feedback

control and without changing the preloading. The magnetic force needs to be large enough to decrease the stress below the reference stress level on its first application and before the muscle contractance curve reaches its peak value (Figure C.2). The value of the necessary force is not determined for all the cases but could be easily found experimentally.

### Control Device II

The second system uses a pump composed of one cylinder containing two separate interacting plungers and springs, both with viscous damping (Figure 1.3(b)). The detailed block diagram of this control method is shown in Figure 1.6: The characteristics and the results of this device are as follows:

1. It was found that in order to accomplish the constant stress level, the second spring (the spring located in the back of the plunger with magnetic control) had to be very rigid. This rigidity causes so little displacement of the second plunger that it could be almost thought of as a rigid wall, which would in effect make this system comparable to the first system of one plunger and one spring (Figure C.7).
2. The feedback control in this method was not as effective as the feedback control in the first concept; that is, the

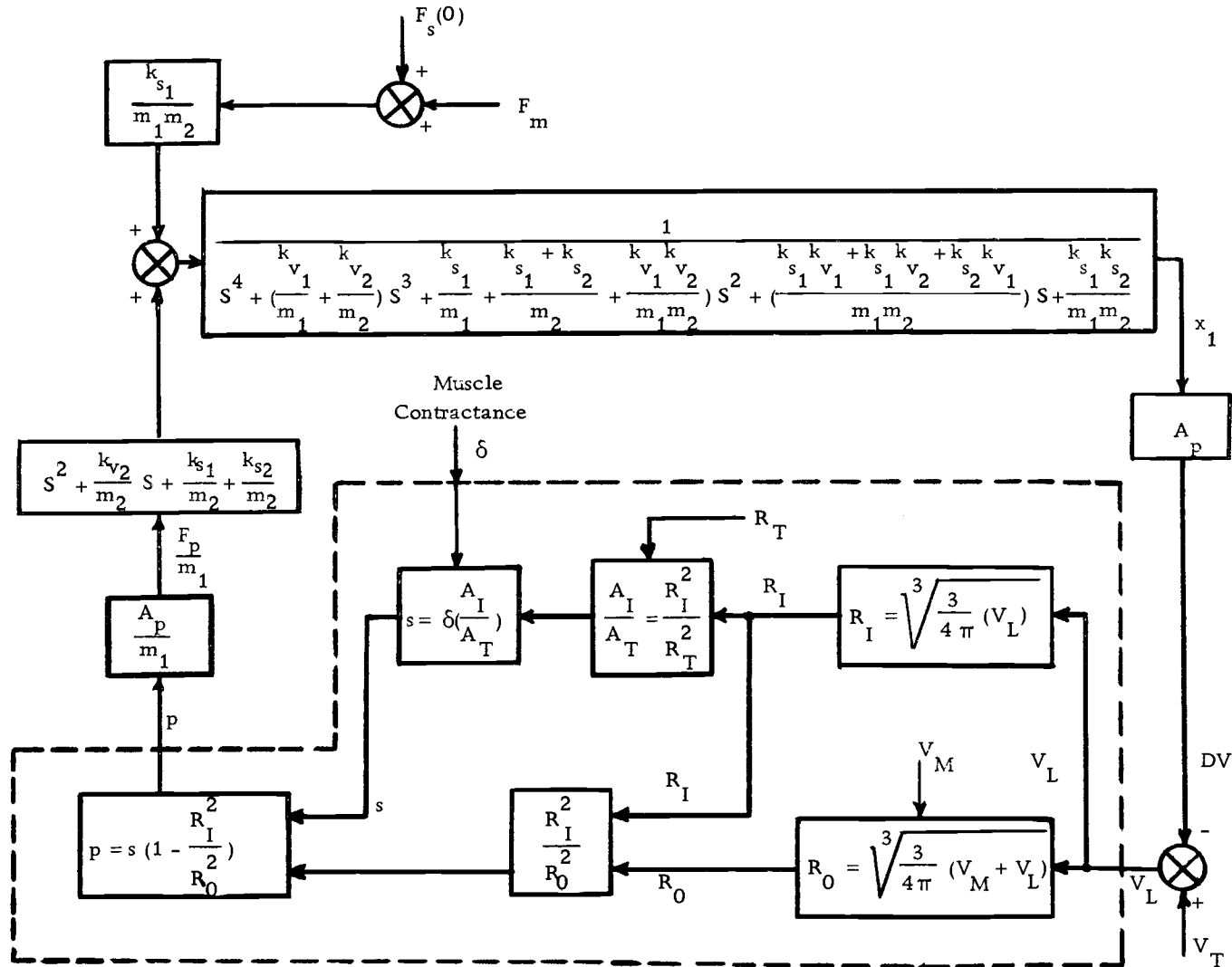


Figure 1. 6. Block diagram of the approximated model of the left ventricle with controlled stress level, using the control device II, on a hybrid computer. (The portion enclosed within the broken line is simulated on the digital computer and the rest on the analog computer.)

effect of control was delayed. Thus the controlled level for the stress profile appears on the obtained graph as a wavy pattern (Figure C. 6). This effect is characterized by a lower frequency and larger magnitude of oscillation around the reference stress level. For the first control device a higher frequency and smaller amplitude of oscillation were achieved.

3. Because of the rigidity of the second spring, the magnetic force had to be ten times as large as the one required in the first system. Compare (Figure C. 4) and (Figure C. 7).

Considering and comparing the overall results of both concepts, the first concept is recommended by the author for further study and possible use. The factors impairing the second control concept are its larger size, larger required control force, wavy stress level control, and greater number of system parameters.

In the course of the research, a model of the left ventricle was simulated on the hybrid computer. There were some assumptions made on the shape, muscle volume, muscle contractance curve, etc., which were explained earlier, (page 4). Briefly, this model presents the left ventricle as a closed cavity: the blood flow through the left ventricle is stopped and the left ventricle is considered to be in the shape of a thick-walled sphere with one small hole. The hybrid computer simulating this model, given muscle contractance,

muscle volume, total volume of the fluid, and position of the piston, will calculate the pressure and stress inside the left ventricle at any time and transfer these values in the form of sampled data to the analog computer.

In the analog computer the calculated stress level is compared to the desired stress level and through the feedback signal the position of the plunger is accordingly adjusted, in such a way as to keep the stress level constant at the desired level.

A Consideration of the Operation of the  
Control Device if Used as an Auxiliary  
Pump to Control the Pressure in the  
Left Ventricle of the Heart

The results showed that the Control Device I, as a passive device, kept the stress level in the left ventricle satisfactorily below a specified level. The original purpose in designing this device was to provide isotonic conditions in the left ventricle of the human heart for the measurements on the heart muscles. Another possible use of this device, seen by the author for the future, is as an auxiliary pump to control the left ventricular pressure. In this section the effect of this device on the circulatory system is compared to the effect of the normal heart operation.

If the Control Device I were connected to the aorta, as shown in Figure 1.7, it would reduce the amount of stress on the aorta and



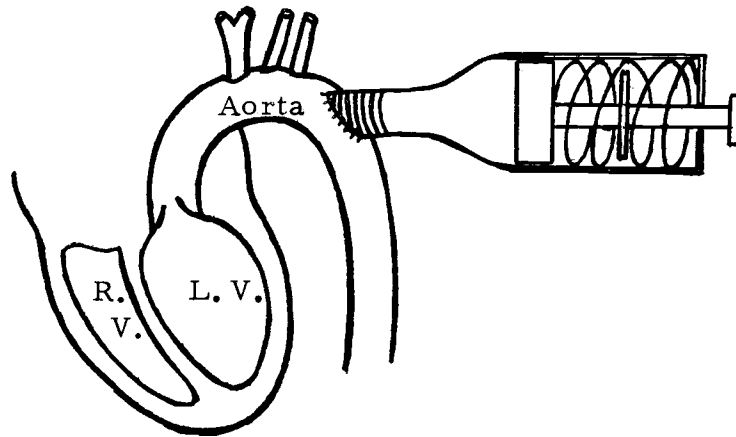


Figure 1.7. Schematic diagram of the possible use of the Control Device I as an auxiliary pump to control the left ventricular pressure.

other immediate blood vessels, but it would not reduce the amount of flow; i. e., the volume of blood supplied to the body by each beat of the heart would remain the same, the only difference being that the flow would be distributed over a longer period of time.

The rate of flow versus time for both the uncontrolled and controlled left ventricle is shown in Figure 1.8. The rate of flow without the control device is shown by the broken line, the area under the broken line being equal to the total amount of blood transferred in one beat. The solid line curve shows the rate of flow when the control device is used. In this case the rate of flow is decreased, but the length of flow is increased and the circulatory system operates at a lower pressure. Note the two cross-hatched areas are equal and represent the amount of blood stored in the piston.

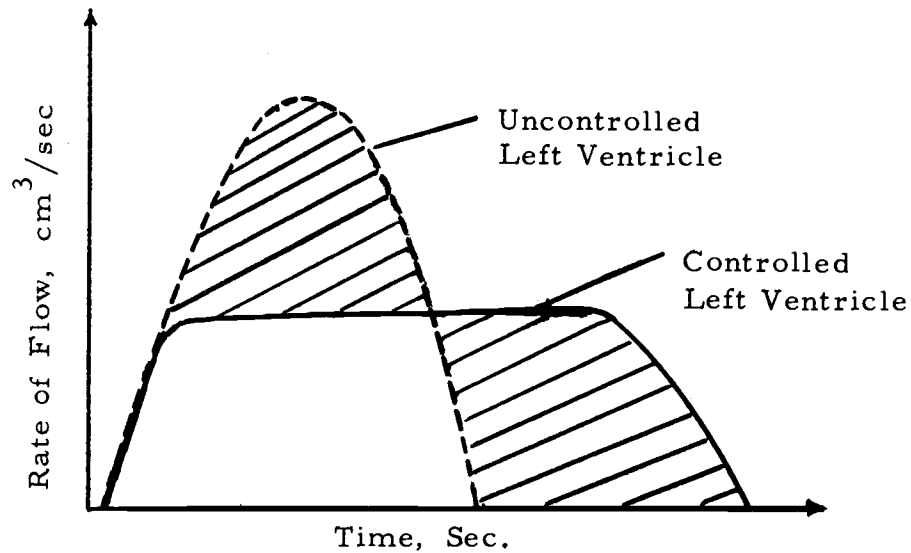


Figure 1.8. Rate of flow versus time for the uncontrolled and controlled left ventricle.

The operation of the circulatory system at lower pressure has been studied by other authors. For example, Jones et al. in their paper titled "Elementary Theory of Synchronous Arterio-Arterial Blood Pumps" (16) consider the effect of withdrawing a volume of fluid from the aorta during the systole (the active period of the heart) and reinjecting during diastole (the inactive period of the heart), thereby reducing the systolic pressure of the heart. The operation of the left ventricle and aorta at lower pressure is considered useful in treatment of patients with failing hearts and is even thought to add energy to the systemic circulation (16). The arterio-arterial pumps suggested in this paper are shown in Figure 1.10.

### Literature Review

In the past very little work has been done on modeling of the left ventricle as a complete system. There are a few articles on isometric measurements on the hearts of animals, but no one has worked on isotonic measurements of the heart muscles.

A short summary of the physiology of the heart is found in Peterson's thesis (19) which provides a good technical background for the understanding of the heart functions, thus eliminating the tedious job of reading the detailed physiological papers.

Some aspects of the muscular contractions discussed by Podolsky in his article (20) are useful in the studies of the heart functions. This article explains the purpose of isometric and isotonic measurements of muscles and their use in obtaining the force velocity curves. These curves, which help in understanding the mechanical and chemical properties of the muscles, lead to the theories on the contraction and structure of the contractile elements of the muscles.

Some research has been done on the isometric measurements (2, 3, 5, 6). However, there are no reports on isotonic measurements on heart muscles.

Isometric contractions are measured on the hearts of rats and larger animals. Strain gauge arches are used for these direct measurements, and synchronous recordings on the contractile force

from different areas of the ventricles are obtained (2, 3, 5, 6).

There are many articles on the simulation of the circulatory system and various organs of the human body on analog computers (12, 13, 17, 22, 23). Dione (8) and Hara (14) consider the cardiovascular system from the hydrodynamic point of view, i. e. the blood flow in and out of a "compartment".

Beneken (1) in his study of the cardiac properties give a mathematical description of the human circulatory system, "in order to build up a proper basis for future investigations on control of the circulation." He describes the circulatory system composed of eight compartments. In order to derive the equation for the left ventricle compartment the left ventricular configuration must be simplified. Beneken makes the following assumption in considering the shape of the left ventricle: "The left ventricular cavity is considered to be bounded by a complete, spherical shell with uniform thickness, and the right ventricular cavity to be bounded by part of the outer surface of the left ventricle together with a spherical free wall bent around a part of the left ventricle" (Figure 1.9).

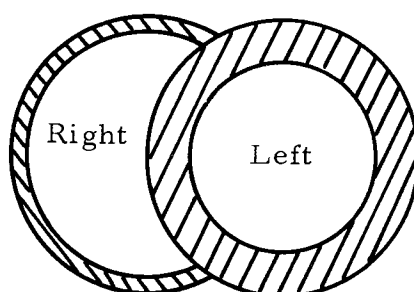


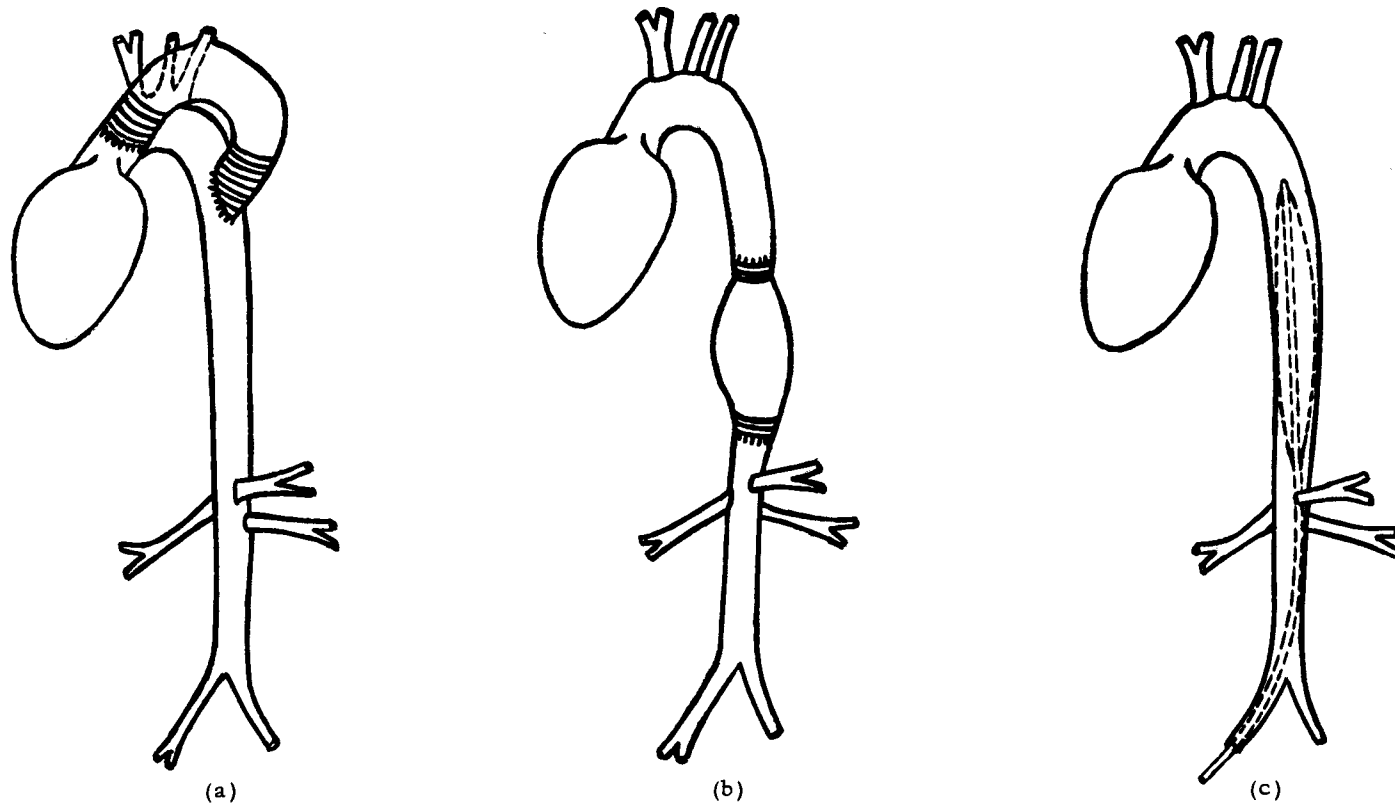
Figure 1.9. Cross-section of the assumed right and left ventricular configuration.

The report on the Mock Circulatory System (15) explains the basic structure of a hydraulic model of the circulatory system used for research on the heart at the National Institute of Health. It may be possible to test the control device designed in this thesis on the Mock Circulatory System.

Jones et al. (16) considers a technique in arterio-arterial pumping in which, "a volume of fluid is withdrawn from the aorta during systole and reinjected during diastole thereby reducing the systole pressure of the heart and adding energy to the systemic circulation." The three methods of pumping are shown in Figure 1.10.

### Recommendations

1. A better approximation of the modeled left ventricle can be achieved if the following items are implemented:
  - a. Consideration of the dynamics of fluid flow from the left ventricular cavity into the pump.
  - b. Development of a more realistic stress profile across the thickness of a spherical shell (21).
  - c. Use of the recorded pulses of the left ventricle of a human heart as the muscle contractance input, instead of use of a DFG for generating the pulses.
2. A better set of parameter constants can be obtained if



- (a) Thoracic auxiliary ventricle
- (b) Auxiliary ventricle in descending aorta
- (c) Intra-aortic balloon pump

Figure 1.10. Arterio-arterial pumps.

the digital computer is used to automate the process of trial and error.

3. The electromagnetic controlling force can be more realistically simulated.
4. The suggested control device should be built and tested in the following two conditions:
  - a. On the Mock Circulatory System (15) hydraulic model of the heart and circulatory system, and
  - b. On animal hearts.

When the device is working successfully, it should be tested on a human heart with the help of a medical advisor, using the method suggested by Covell (7, Appendix D).

## II. MODEL OF THE LEFT VENTRICLE OF THE HUMAN HEART

Isometric and isotonic measurements on the cardiac muscles must be obtained from a live heart (2). A control device is needed to keep a constant stress level during a portion of the systole <sup>1/</sup> in the left ventricle so that the measurement devices can obtain the data for isotonic conditions of the heart structure. Since a live human heart is impractical at this stage, a model of a live heart is used in this thesis.

After lengthy study and evaluation of the influences of the different cavities of the heart on each other, Beneken (1) comes to the conclusion that, as far as the heart muscle is concerned, the operation of the left ventricle (due to the thickness of the muscle surrounding the left ventricular cavity and its shape) is more or less independent of the rest of the heart. This conclusion is assumed valid in this thesis. Therefore, only the left ventricle of the heart needs to be modeled.

---

<sup>1/</sup> 1. "The usual rhythmic contraction of the heart, especially of the ventricles, following each dilatation (diastole), during which the blood is driven onward from the chambers." (Webster's New World Dictionary of the American Language, 1960 Edition)

2. "The heart's period of mechanical activity is known as systole" (19).



### Shape of the Left Ventricle

The shape of the left ventricle is an important element in the study of its muscle properties. Beneken (1) states "the left ventricular cavity is more or less egg-shaped. During the initial, isovolumic <sup>2/</sup> part of the ventricular systole, the length axis of the left ventricle shortens and the diameters increase, resulting in a more spherical shape".

Studies have been made in which the left ventricle is assumed to be a cylinder with a variable cross-section and constant length, but this model of the left ventricle requires modifications in order to attain satisfactory values of the variables. Beneken (1) considers the left ventricular cavity to be bounded by a complete, spherical shell with uniform thickness. The characteristics of this model approach that of the actual left ventricle. The spherical model is therefore adopted in this thesis.

---

<sup>2/</sup> "The onset of systole is initiated by the contraction of the atria which propels additional blood into the ventricles. Within two-tenths of a second the ventricles begin to contract and thereby cause a rise in ventricular pressure. This pressure shuts the atrioventricular valves, and with further contraction the pressure continues to rise. Since all the valves are shut, the ventricular volume remains constant, and this is known as the period of isometric (isovolumic) contraction" (19).

### Muscle Surrounding the Left Ventricular Cavity

The muscle surrounding the left ventricular cavity is assumed to be a thick-walled spherical shell (1). The assumption is made that the volume of this muscle stays constant. On this point Beneken makes the following remarks:

"Based on the high water content of all the tissues, the assumption is made that the wall material is incompressible; thus, contraction will result in an increase in wall thickness. We discard a possible fluid exchange, during the course of one cardiac cycle."

Beneken makes further assumptions which are useful in the case of the "normal, closed, uncontrolled circulatory system in which gravitational influences are not considered." These assumptions are not used in this study, since they are not applicable for the studies considered in this thesis.

### Muscle Contractance Curve

In order to complete the feedback loop in the control system either a pressure transducer or a stress measuring device is needed in the actual open-heart surgery; and since the heart must be operating, the muscles would continue to contract and expand due to the excitation signals sent to the heart cavities (7, Appendix D). The contraction and expansion of the muscles are the cause of the pressure change in the cavities.

In modeling the left ventricle the pressure changes in this cavity should be comparable to the actual pressure profile of the left ventricle. To accomplish this in our model of the left ventricle, a signal is generated by a DFG (diode function generator) which is referred to as the muscle contractance curve. This curve is similar in shape to the pressure profile of the left ventricle (Figure A. 1). In order to obtain the stress on the walls of the left ventricle, the muscle contractance signal is multiplied by the ratio  $\frac{A_I}{A_T}$ , where  $A_I$  represents the internal area of the left ventricular cavity and  $A_T$  represents the internal area when the left ventricle is at rest and completely filled with fluid, therefore

$$s = \delta \frac{A_I}{A_T} \quad (2.1)$$

where  $\delta$  is the muscle contractance signal. Such a relation for stress is chosen since the tension on the walls of the left ventricle is proportional to the size of the cavity or the amount of stretch in the muscles. For more information on the generation of  $\delta$  refer to Appendix A.

### Derivation of Formulae Leading to Pressure Calculation

#### a. Volume of Fluid in the Left Ventricular Cavity

The position of the plunger, connected to the left ventricle

(Figure 1.1),  $x$ , determines the volume of the fluid withdrawn from the left ventricular cavity,  $DV$ , as given by the following relation:

$$DV = x \cdot A_p \quad (2.2)$$

where  $A_p$  is the cross-sectional area of the piston. Then the volume of the fluid inside the left ventricle,  $V_L$ , can be obtained, knowing the total volume of the fluid in the system  $V_T$ .

$$V_L = V_T - DV \quad (2.3)$$

The value of  $V_L$  is digitized and transferred to the digital computer using an ADC (analog digital converter).

#### b. Internal and External Radii of the Left Ventricle

Knowing the left ventricle muscle volume,  $V_M$ , the internal and the external radii of the left ventricle can be calculated, using the following relations:

$$V_L = \frac{4}{3} \pi R_I^3 \quad (2.4)$$

$$V_L + V_M = \frac{4}{3} \pi R_O^3 \quad (2.5)$$

where  $R_I$  = internal radius of the left ventricle

$R_O$  = external radius of the left ventricle.

From the Equations (2.4) and (2.5), the relations for the  $R_I$  and  $R_O$  in terms of  $V_L$  and  $V_M$  can be derived:

$$R_I = \sqrt[3]{\frac{3}{4\pi} V_L} \quad (2.6)$$

$$R_O = \sqrt[3]{\frac{3}{4\pi} (V_L + V_M)} \quad (2.7)$$

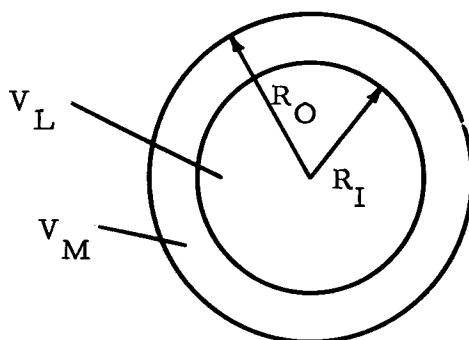


Figure 2.1. Cross-section of the left ventricular cavity.

### c. Wall Stress

The wall stress in a spherical shell is not constant throughout the cross-section of the muscle and the maximum wall stress occurs on the internal wall of the shell (21), (Figure 2.2).

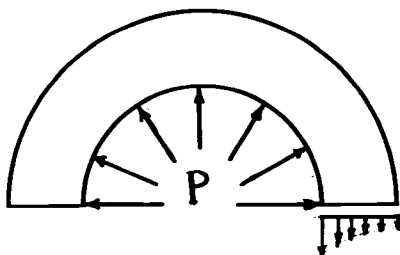


Figure 2.2. Stress profile in the muscle cross-section.

The stress is a three-dimensional vector; the tangential component of the stress is derived by Flügge (1) to be:

$$T_{\text{tang}} = P \frac{r_i^3 (2r_o^3 + r_i^3)}{2r_o^3 (r_o^3 - r_i^3)} \quad (2.8)$$

Beneken (1) states that the above formula is "derived for an isotropic wall material with constant modulus of elasticity. Heart muscle certainly has no such properties."

Beneken derives the following formula for the stress in the walls of the left ventricle:

$$T_{\text{tang}} = P_{\text{LV}} \frac{4r_i^3 + r_i^2 r_o + r_i r_o^2}{4(r_o^3 - r_i^3)} \quad (2.9)$$

For the purposes of this study it is assumed that the stress is constant throughout the wall and is derived in a less rigorous manner to be the force per unit area of the cross section of the wall.

The stress on the walls of the left ventricle is defined as follows:

$$\begin{aligned} \text{Stress} &= \frac{(\text{Pressure})(\text{Base area of the cross-section})}{\text{cross-sectional area of the muscle}} \\ &= \frac{P(\pi R_O^2)}{\pi (R_O^2 - R_I^2)} \end{aligned} \quad (2.10)$$

Therefore

$$s = \frac{P R_O^2}{R_O^2 - R_I^2} \quad (2.11)$$

d. Pressure

Since the stress is obtained from Equation (2.1), the pressure can be calculated in terms of the stress. The rearranged formula will be:

$$P = \frac{R_O^2 - R_I^2}{R_O^2} \cdot s \quad (2.12)$$

The block diagram illustrating the total intercorrelation of the above-listed formulae, modeling the left ventricle and the control method is shown in Figure 1.4.

### III. CONTROL DEVICES

A control device is developed to keep the stress in the left ventricle of the human heart below a certain level. This device needs to be modeled on an analog computer in order to connect it to the hybrid computer model of the left ventricle discussed in Chapter II.

Two control devices, shown in Figure 1.3., are to be modeled and tested. Differential equations of these devices are needed in order to model them on an analog computer. Derivation of the differential equations for the two proposed control devices are shown below.

#### Control Device I

This device is a simple mechanical system, as shown in Figure 1.3(a); in order to derive the corresponding differential equation the summation of all forces present in the system are set equal to zero in Equation (3.7). The forces present are as follows:

a. the inertial force

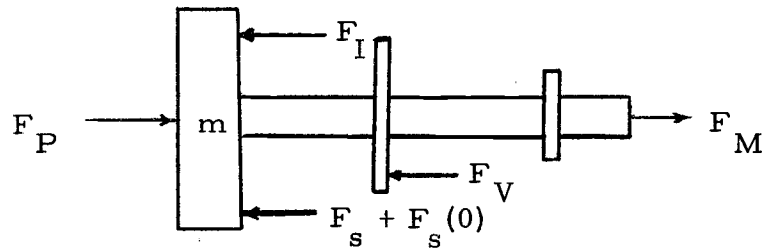
$$F_I = + m\ddot{x} \quad (3.1)$$

where  $m$  = mass of the mechanical system in motion.

$x$  = displacement of the piston

and  $\ddot{x} = \frac{d^2 x}{dt^2}$  acceleration of the piston.



Figure 3.1. Free-body diagram of  $m$ .

b. the friction or damping force due to the viscous force of the dash-pot and the friction between the piston and the cylinder.

$$F_v = + (k_f + k_v) \dot{x} \quad (3.2)$$

where  $k_f$  = friction coefficient

$k_v$  = viscous damping coefficient

and  $\dot{x} = \frac{dx}{dt}$  velocity of the piston,

c. the force of the spring

$$F_s = + k_s x \quad (3.3)$$

where  $k_s$  = spring constant,

d. force on the piston due to the pressure inside the left ventricle

$$F_p = PA_p \quad (3.4)$$

where  $P$  = pressure inside the left ventricle

$A_p$  = area of the piston,

e. force of the electromagnet applied to the plunger

$$F_m = f(i) \quad (3.5)$$

where  $i$  = current in the coil of the electromagnet

$$f. F_s(0) = \text{constant}$$

where  $F_s(0) = \text{constant}$  preloading force of the spring

$$+ F_I + F_v + F_s + F_s(0) = F_p + F_m \quad (3.7)$$

$$m\ddot{x} + (k_f + k_v)\dot{x} + k_s x = PA_p + F_m - F_s(0) \quad (3.8)$$

$$\ddot{x} = -\frac{k_f + k_v}{m}(\dot{x}) - \frac{k_s}{m}(x) + \frac{A_p}{m}P + \frac{F_m}{m} - \frac{F_s(0)}{m} \quad (3.9)$$

Using the Laplace transformation the above equation could be obtained in terms of the transfer function times the inputs.

$$X = \left[ \frac{1}{mS^2 + (k_f + k_v)S + k_s} \right] [PA_p + F_m - F_s(0)] \quad (3.10)$$

Knowing the transfer function of the control system and using the equations derived in Chapter II which describe the left ventricle, the block diagram of the whole system employing the first method of control can be drawn as shown in Figure 1.4.

Due to the extensive range of variation corresponding to the variables in Equation (3.9), this equation cannot be directly simulated on an analog computer. However, the simulation is made possible by magnitude and time scaling, which keeps the variation of voltages representing the variables within the limits of the amplifier's operation.

### Magnitude Scaling

Magnitude scaling is done by normalizing each variable; i.e., each variable is divided by its maximum value and the new variable is substituted in the equation. The new variables are:

$$\begin{aligned}
 e_x &= \frac{x}{10} & e_f &= \frac{F_m}{10^7} & e_{f_s}(0) &= \frac{F_s(0)}{10^7} \\
 e_{\dot{x}} &= \dot{x} & e_s &= \frac{s}{10^7} & & \\
 e_p &= \frac{P}{10^7} & e_{v_t} &= \frac{V_T}{100} & &
 \end{aligned} \tag{3.11}$$

(e's signify the voltages in the analog computer.) After substitution the Equation (3.9) would become:

$$\begin{aligned}
 e_{\ddot{x}} &= - \frac{k_v + k_f}{m} (\dot{x}) + \frac{10k_s}{m} \left( \frac{x}{10} \right) + \frac{10^7 A_P}{m} \left( \frac{P}{10^7} \right) \\
 &\quad + \frac{10^7}{m} \left( \frac{F_m}{10^7} - \frac{F_s(0)}{10^7} \right)
 \end{aligned} \tag{3.12}$$

The magnitude scaled equation of the system is:

$$e_{\ddot{x}} = - \frac{k_v + k_f}{m} e_{\dot{x}} + \frac{10k_s}{m} e_x + \frac{10^7 A_P}{m} e_p + \frac{10^7}{m} [e_f - e_{f_s}(0)] \tag{3.13}$$

### Time Scaling

Time scaling permits solution of differential equations on an analog computer at a slower or a faster rate compared to real time.

In this thesis the problem is solved at a rate 1000 times slower than real time. This slower rate increases the number of samples made available to the digital computer from each cycle (heartbeat) and results in greater accuracy.

The relationship between real time and computer time, using  $\eta$  to represent the time scaling factor, is as follows:

$$t = \frac{T}{\eta} \quad (3.14)$$

where  $t$  = real time

$T$  = computer time

In terms in Equation (3.13) which involve real time should be replaced by new terms representing the computer time. The derivation of the new terms is as follows:

$$\dot{x} = \frac{dx}{dt} = \frac{dx}{d(\frac{T}{\eta})} = \eta \frac{dx}{dT} \quad (3.15)$$

$$\ddot{x} = \frac{d^2x}{dt^2} = \frac{d^2x}{d(\frac{T}{\eta})^2} = \eta^2 \frac{d^2x}{dT^2} \quad (3.16)$$

Substituting these relations in Equation (3.13) and simplifying the equation results in the magnitude and time-scaled differential equation of the system:

$$e_{\ddot{x}} = - \frac{k_v + k_f}{m\eta} e_{\dot{x}} - \frac{10k_s}{m\eta^2} e_x + \frac{10^7 A_p}{m\eta^2} e_p + \frac{10^7}{m\eta^2} [e_f - e_{f(0)}] \quad (3.17)$$

The whole system was modeled and tested on a hybrid computer. The diagram for setting up the hybrid computer system EAI 690 is shown in the Figures B.1 and B.3. Note, since  $k_f$  is very small compared to  $k_v$  it is omitted in the simulations.

### Parameter Values

For modeling of the Control Device I on an analog computer, several pots are used. For each pot setting an equation is derived in terms of the unknown parameters. (Refer to Table B.1 for these relations.) Originally some approximate values for the parameters were used to scale the system equations to fit them to the computer. When this system was simulated and debugged, the pot values were adjusted until the most desirable results were obtained. These new values of the pot settings are used to calculate the parameters for the control device from the pot equations (Table B.1).

There is one less equation than the number of unknowns. Thus if there is any restriction to the size or weight of the device, one of the parameters can be chosen at will to meet the requirements and the rest of the parameters are then fixed by the relations. In this case  $A_p$ , the piston area, is chosen to be  $10 \text{ cm}^2$ , and the rest of the parameters are determined by the relations given in Table B.1. The parameter values which would provide a good starting point for the follow-up research in this area are written below:

$$A_p = 10 \text{ cm}^2$$

$$m = 100 \text{ grams}$$

$$k_s = 7 \times 10^6 \text{ dynes/cm}$$

$$k_v = 10^5 \text{ dynes/cm/sec}$$

$$F_m = 10^7 \text{ dynes}$$

$$s_{\text{ref}} = 5.7 \times 10^6 \text{ dynes/cm}^2$$

$$F_s(0) = 10^5 \text{ dynes}$$

$$\begin{array}{llll} \text{PO6} = .143, & R_T = 2.42, & V_m = 70 \text{ cm}^3, & V_T = 60 \text{ cm}^3 \\ \text{PO6} = .2286, & R_T = 2.88, & V_m = 150 \text{ cm}^3, & V_T = 100 \text{ cm}^3 \\ \text{PO6} = .358, & R_T = 3.3, & V_m = 170 \text{ cm}^3, & V_T = 150 \text{ cm}^3 \end{array}$$

### Control Device II

This device is a pump composed of one cylinder which contains two separate interacting plungers and springs, with both plungers having viscous damping, as shown in Figure 1.3(b).

To obtain the differential equations of this control device the free-body diagrams are considered. The forces exerted on the first body are shown in Figure 3.2. The force of friction compared to the

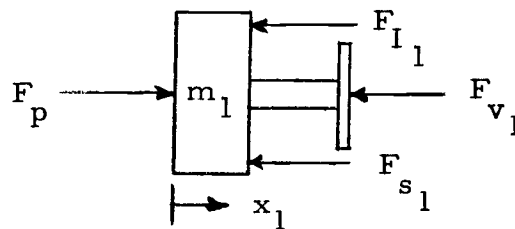


Figure 3.2. Free-body diagram of  $m_1$ .

viscous damping force is negligible. When the sum of all the forces in this free body diagram is set equal to zero the following relation results:

$$F_p = F_{I_1} + F_{v_1} + F_{s_1} \quad (3.18)$$

After substitution and rearrangement the following relation is obtained:

$$\ddot{x}_1 = -\frac{k_{v_1}}{m_1} \dot{x}_1 - \frac{k_{s_1}}{m_1} (x_1 - x_2) + \frac{A_p}{m_1} P \quad (3.19)$$

The forces exerted on the second body are shown in Figure

3.3.

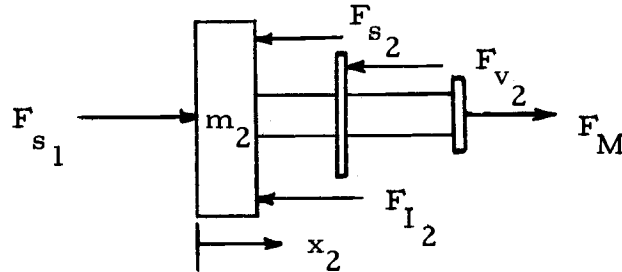


Figure 3.3. Free-body diagram of  $m_2$ .

Equating sum of the forces to zero, results in:

$$F_{s_1} + F_m = F_{I_2} + F_{v_2} + F_{s_2} + F_s(0) \quad (3.20)$$

or, after substitution and rearrangement:

$$\ddot{x}_2 = -\frac{k_{v_2}}{m_2} \dot{x}_2 - \left(\frac{k_{s_1}}{m_2} + \frac{k_{s_2}}{m_2}\right) x_2 + \frac{k_{s_1}}{m_2} x_1 + \frac{F_m}{m_2} - \frac{F_s(0)}{m_2} \quad (3.21)$$

The equations of the system are transformed from time domain into frequency domain by the use of Laplace transformation. This process provides the transfer function of the system which is used in the block diagram of the control system, shown in Figure 1.6.

The two equations are transformed, simplified and solved for  $X_1(s)$  as follows:

$$X_1(s)S^2 = -\frac{k_{v1}}{m_1} X_1(s)S - \frac{k_{s1}}{m_1} [X_1(s) - X_2(s)] + \frac{A}{m_1} P \quad (3.22)$$

$$X_2(s)S^2 = -\frac{k_{v2}}{m_2} X_2(s)S - \left(\frac{k_{s1}}{m_2} + \frac{k_{s2}}{m_2}\right)X_2(s) + \frac{k_{s1}}{m_2} X_1(s) + \frac{F_m - F_s(0)}{m_2} \quad (3.23)$$

Using Equation (3.23)

$$X_2(s) = \frac{\frac{k_{s1}}{m_2} X_1(s) + \frac{F_m}{m_2} - \frac{F_s(0)}{m_2}}{S^2 + \frac{k_{v2}}{m_2} S + \left(\frac{k_{s1}}{m_2} + \frac{k_{s2}}{m_2}\right)} \quad (3.24)$$

Substituting for  $X_2(s)$  in Equation (3.22)

$$X_1(s)S^2 = -\frac{k_{v1}}{m_1} X_1(s)S - \frac{k_{s1}}{m_1} X_1(s) + \frac{k_{s1}}{m_1} \left[ \frac{\frac{k_{s1}}{m_2} X_1(s) + \frac{F_m}{m_2} - \frac{F_s(0)}{m_2}}{S^2 + \frac{k_{v2}}{m_2} S + \left(\frac{k_{s1}}{m_2} + \frac{k_{s2}}{m_2}\right)} \right] + \frac{A}{m_1} P \quad (3.25)$$



Solving for  $X_1(s)$

$$\begin{aligned}
 X_1(s) = & \frac{\frac{A_p}{m_1} P \left[ S^2 + \frac{k_{v2}}{m_2} S + \frac{k_{s1}}{m_2} + \frac{k_{s2}}{m_2} \right] +}{S^4 + \left( \frac{k_{v1}}{m_1} + \frac{k_{v2}}{m_2} \right) S^3 + \left( \frac{k_{s1}}{m_1} + \frac{k_{s1}}{m_2} + \frac{k_{s2}}{m_2} + \frac{k_{v1} k_{v2}}{m_1 m_2} \right) S^2 +} \dots \\
 & + \frac{\frac{k_{s1}}{m_1 m_2} [F_m - F_s(0)]}{\dots} \\
 & + \left( \frac{k_{s1} k_{v1}}{m_1 m_2} + \frac{k_{s1} k_{v2}}{m_1 m_2} + \frac{k_{s2} k_{v1}}{m_1 m_2} \right) S + \frac{k_{s1} k_{s2}}{m_1 m_2}
 \end{aligned} \tag{3.26}$$

Knowing the transfer function of the second control method and equations derived in Chapter II which describe the left ventricle, the block diagram of the whole system may be drawn as shown in Figure 1.6.

Equations (3.19) and (3.21) are the system equations and need to be scaled for the simulation on the analog computer.

### Magnitude Scaling

The same procedure as the one used to scale the differential equation in the control system I is used here to scale the equations of the second system.

The new normalized variables for the second system are:

$$\begin{aligned}
e_{x_1} &= \frac{x_1}{10} & e_{x_2} &= \frac{x_2}{10} \\
e_{\dot{x}_1} &= \dot{x}_1 & e_{\dot{x}_2} &= \dot{x}_2 \\
e_{\ddot{x}_1} &= \ddot{x}_1 & e_{\ddot{x}_2} &= \ddot{x}_2 \\
e_p &= \frac{P}{10^7} & e_f &= \frac{F_m}{10^7} \\
e_s &= \frac{s}{10^7} & e_{v_T} &= \frac{V_T}{100} \\
e_{f_s(0)} &= \frac{F_s(0)}{10^7}
\end{aligned} \tag{3.27}$$

The magnitude scaled equations of this system then become:

$$e_{\ddot{x}_1} = -\frac{k_{v_1}}{m_1} e_{\dot{x}_1} - \frac{10^7 k_{s_1}}{m_1} (e_{x_1} - e_{x_2}) + \frac{10^7 A_p}{m_1} e_p \tag{3.28}$$

$$e_{\ddot{x}_2} = -\frac{k_{v_2}}{m_2} e_{\dot{x}_2} - \left(\frac{k_{s_1}}{m_2} + \frac{k_{s_2}}{m_2}\right) 10 e_{x_2} + \frac{10^7 k_{s_1}}{m_2} e_{x_1} + \frac{10^7}{m_2} [e_f - e_{f_s(0)}] \tag{3.29}$$

These equations also need to be time scaled.

### Time Scaling

The Equations (3.28) and (3.29) after time scaling would give us the following equations:

$$e_{\ddot{x}_1} = -\frac{k_{v_1}}{m_1 \eta} e_{\dot{x}_1} - \frac{10^k s_1}{m_1 \eta^2} (e_{x_1} - e_{x_2}) + \frac{10^7 A_p}{m_1 \eta^2} e_p \quad (3.30)$$

$$e_{\ddot{x}_2} = -\frac{k_{v_2}}{m_2 \eta} e_{\dot{x}_2} - \left(\frac{k_{s_1}}{m_2} + \frac{k_{s_2}}{m_2}\right) \left(\frac{10}{\eta^2}\right) e_{x_2} + \frac{10^k s_1}{m_2 \eta^2} e_{x_1} + \frac{10^7}{m_2 \eta^2} [e_f - e_{f_s(0)}] \quad (3.31)$$

This system also will be solved at a rate 1000 times slower than real time. Thus when  $\eta = 1000$  the Equations (3.30) and (3.31) simplify into the following equations:

$$e_{\ddot{x}_1} = -\frac{10^{-3} k_{v_1}}{m_1} e_{\dot{x}_1} - \frac{10^{-5} k_{s_1}}{m_1} (e_{x_1} - e_{x_2}) + \frac{10 A_p}{m_1} e_p \quad (3.32)$$

$$e_{\ddot{x}_2} = -\frac{10^{-3} k_{v_2}}{m_2} e_{\dot{x}_2} - \left(\frac{k_{s_1}}{m_2} + \frac{k_{s_2}}{m_2}\right) (10^{-5}) e_{x_2} + \frac{10^{-5} k_{s_1}}{m_2} e_{x_1} + \frac{10}{m_2} [e_f - e_{f_s(0)}] \quad (3.33)$$

Equations (3.32) and (3.33) are the magnitude and time scaled differential equations of the second control system.

### Parameter Values

The final values of the parameters for the second control device were obtained through the same process as was used in the case of the first control method. The relations from which the parameters are obtained are shown in Table B.2.

The parameter values are the following:

$$A_p = 10 \text{ cm}^2$$

$$m_1 = 100 \text{ grams}$$

$$k_{s_1} = 5 \times 10^5 \text{ dynes/cm}$$

$$k_{v_1} = 5 \times 10^4 \text{ dynes/cm/sec}$$

$$m_2 = 20 \text{ grams}$$

$$k_{s_2} = 8 \times 10^6 \text{ dynes/cm}$$

$$k_{v_2} = 1.99 \times 10^5 \text{ dynes/cm/sec}$$

$$F_m = 6 \times 10^6 \text{ dynes}$$

$$F_s(0) = 2 \times 10^5 \text{ dynes}$$

$$V_T = 100 \text{ cm}^3$$

$$s_{\text{ref}} = 5.4 \times 10^6 \text{ dynes/cm}^2$$

## BIBLIOGRAPHY

1. Beneken, J. E. W. A mathematical approach to cardiovascular function. (Reprint)
2. Bir̄o, A., M. Rusn̄akova and J. Rusn̄ak. A device for measuring isometric contractions mechanoelectrically. *Physiologia Bohemoslovenica* 15:391-394. 1964.
3. Boniface, K. J., O. J. Brodie and R. P. Walton. Resistance strain gauge arches for direct measurement of heart contractile force in animals. *Proceedings of the Society for Experimental Biology and Medicine* 84:263-266. 1953.
4. Brecher, Gerhard A. and Pierre M. Gilletti. Functional anatomy of cardiac pumping. In: *Handbook of physiology. Sec. 2. Circulation. Vol. 2.* Washington, D. C., American Physiological Society, 1962. p. 759-798.
5. Cotton, Marion DeV. Circulatory changes affecting measurement of heart force in situ with strain guage arches. *American Journal of Physiology* 174:365-370. 1953.
6. Cotton, Marion DeV. and Edmund Ray. Direct measurement of changes in cardiac contractile force, relationship of such measurements to stroke work, isometric pressure gradient and other parameters of cardiac function. *American Journal of Physiology* 187:122-134. 1956.
7. Covell, James W. National Heart Institute, Cardiology Branch. Letter to Dr. John L. Saugen, Oregon State University, Corvallis. Bethesda, Maryland. June 30, 1967.
8. Dionne, Paul J. and Charles R. Cole. A computer simulation of the human cardiovascular system. Richland, Washington, 1968. 7 p. (Battelle Memorial Institute. BNWL-Sa-1588) (Reprint )
9. Electronic Associates Incorporated. An analog program for electroencephalographic data analysis. West Long Branch, New Jersey, 1965. 4 p. (Applications Reference Library. General purpose analog computation. Bio-medical Application Study 4.4.6a)

10. Electronic Associates Incorporated. A one-organ chemotherapy model. West Long Branch, New Jersey, 1964. 2 p. (Applications Reference Library. General purpose analog computation. Bio-medical Application Notes 4.3.5a)
11. Electronic Associates Incorporated. Hybrid computer analysis of electrocardiographic data. West Long Branch, New Jersey, 1964. 6 p. (Applications Reference Library. Hybrid computation. Bio-medical Application Study 4.4.1h)
12. Guyton, Arthur C., Howard T. Milhorn, Jr. and Thomas G. Coleman. Simulation of physiological mechanisms. Part I. Simulation 9:15-20. 1967.
13. Guyton, Arthur C., Howard T. Milhorn, Jr. and Thomas G. Coleman. Simulation of physiological mechanisms. Part II. Simulation 9:73-79. 1967.
14. Hara, Hiroshi. Analog simulation of ventricular pump action. In: Handbook of analog computation, ed. by Maxwell C. Gilliland. Concord, California, Systron-Donner Corporation. p. 21-1 - 21-4.
15. Hydrospace Research Corporation. Final report on the mock circulatory system. Rockville, Maryland, 1967. Various paging. (Report 152 on Contract PH-43-64-78 prepared for the National Heart Institutes, U. S. National Institute of Health, April 15, 1967)
16. Jones, Robert T., Harry E. Petschek and Arthur R. Kantrowitz. Elementary theory of synchronous arterio-arterial blood pumps. Everett, Massachusetts, 1967. 10 p. (AVCO Everett Research Laboratory. Research Report 272)
17. Lewis, Benjamin M. An "electronic lung" in the study of pulmonary function. Simulation 7:311-323. 1966.
18. McLeod, John. Physbe ... a physiological simulation benchmark experiment. Simulation 7:324-330. 1966.
19. Peterson, Walter Anton. A vector electrocardioscope system for clinical studies. Master's thesis. Corvallis, Oregon State University, 1965. 222 numb. leaves.

20. Podolsky, Richard J. Mechanochemical basis of muscular contraction. Federation Proceedings 21:964-979. 1962.
21. Popov, E. P. Mechanics of materials. Englewood Cliffs, New Jersey, Prentice Hall, 1964. 441 p.
22. Topham, W. Sanford. An analog model of the control of cardiac output. Simulation 8:49-53. 1967.
23. Warner, Homer R. Control of the circulation as studied with analog computer technics. In: Handbook of physiology. Sec. 2. Circulation. Vol. 3. Washington D. C., American Physiological Society, 1962. p. 1825-1842.
24. Wiggers, Carl J. The circulation and circulation research in perspective. In: Handbook of physiology. Sec. 2. Circulation. Vol. 1. Washington, D. C., American Physiological Society, 1962. p. 1-10.

## APPENDICES



## APPENDIX A

GENERATION OF THE MUSCLE CONTRACTANCE CURVE  
BY A DIODE FUNCTION GENERATOR

A DFG (Diode Function Generator) is used to generate the pulses of the left ventricle, which in this thesis are represented by the muscle contractance curve,  $\delta$ . The frequency of the  $\delta$  should be 2 hz (7, Appendix D) since the active state of the heart, i.e., the period during which the left ventricle pumps the blood, lasts for 300 ms. and the left ventricle rests for 200 ms., (Figure A.1), (4, 7).

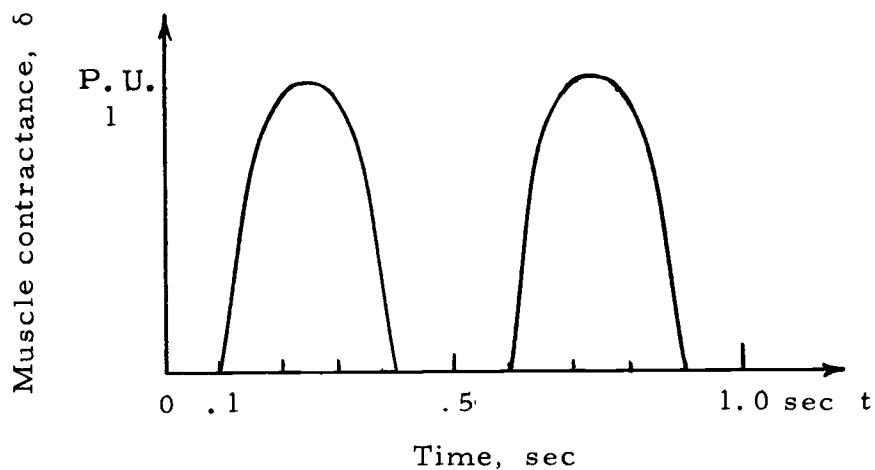


Figure A.1. Muscle contractance curve,  $\delta$ .

To generate such a function a triangular wave of 1 hz which varies between 0 and +1 pu is necessary as the input to the DFG. A triangular wave generator is designed on the analog computer to meet these specifications. The analog computer diagram is shown in Figure A.2.

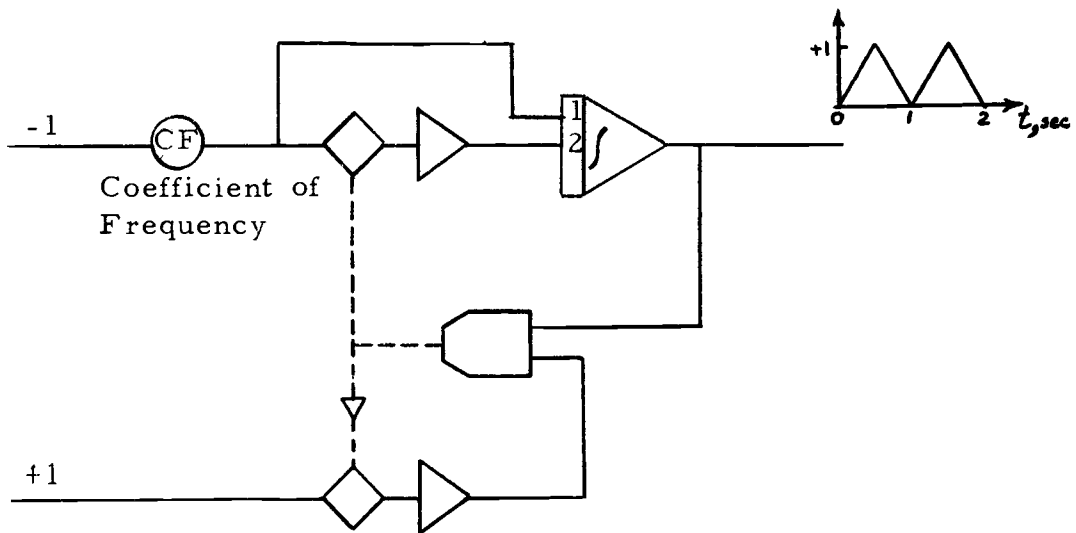


Figure A. 2. Analog computer diagram of a triangular wave generator.

The frequency of the triangular wave can be adjusted by the value of the pot  $CF = \frac{1}{\eta}$ , where  $\eta$  = time scaling factor.

The block diagram showing the generation of  $\delta$  is shown in Figure A. 3.

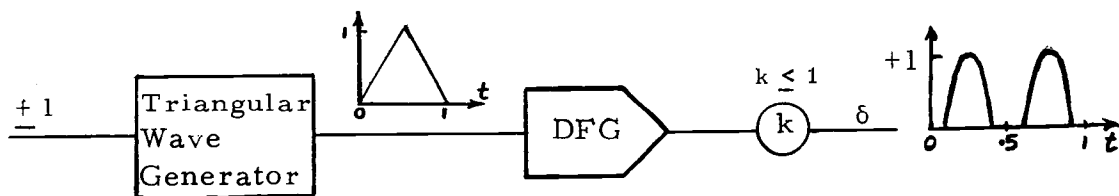


Figure A. 3. Block diagram for the generation of muscle contractance curve,  $\delta$ .

Since the problem on the computer is time scaled to operate at a rate 1000 times slower than the real time the pot setting for  $CF = \frac{1}{\eta} = .001$ .

In this investigation a 10 segment positive DFG in the EAI 680 Analog computer is used and the settings for the generation of  $\delta$  are shown in Table A. 1.

Table A. 1. DFG settings for the generation of  $\delta$  .

DFG	X	Y
0	0.00	0.00
1	0.20	0.00
2	0.26	0.14
3	0.38	0.80
4	0.43	0.94
5	0.50	1.00
6	0.57	0.94
7	0.62	0.80
8	0.74	0.14
9	0.80	0.00
10	1.00	0.00

## APPENDIX B

ANALOG AND DIGITAL COMPUTER DIAGRAMS

On the following pages are shown Analog computer diagrams of the two control methods with Tables showing the Pot settings on EAI 680, and the Digital computer flow diagram with the program modeling the left ventricle. The Analog computer diagrams (Figures B.1, B.2) are drawn in such a way that they can be put next to the Digital flow diagram (Figure B.3) to show the complete hybrid computer model of the control systems.

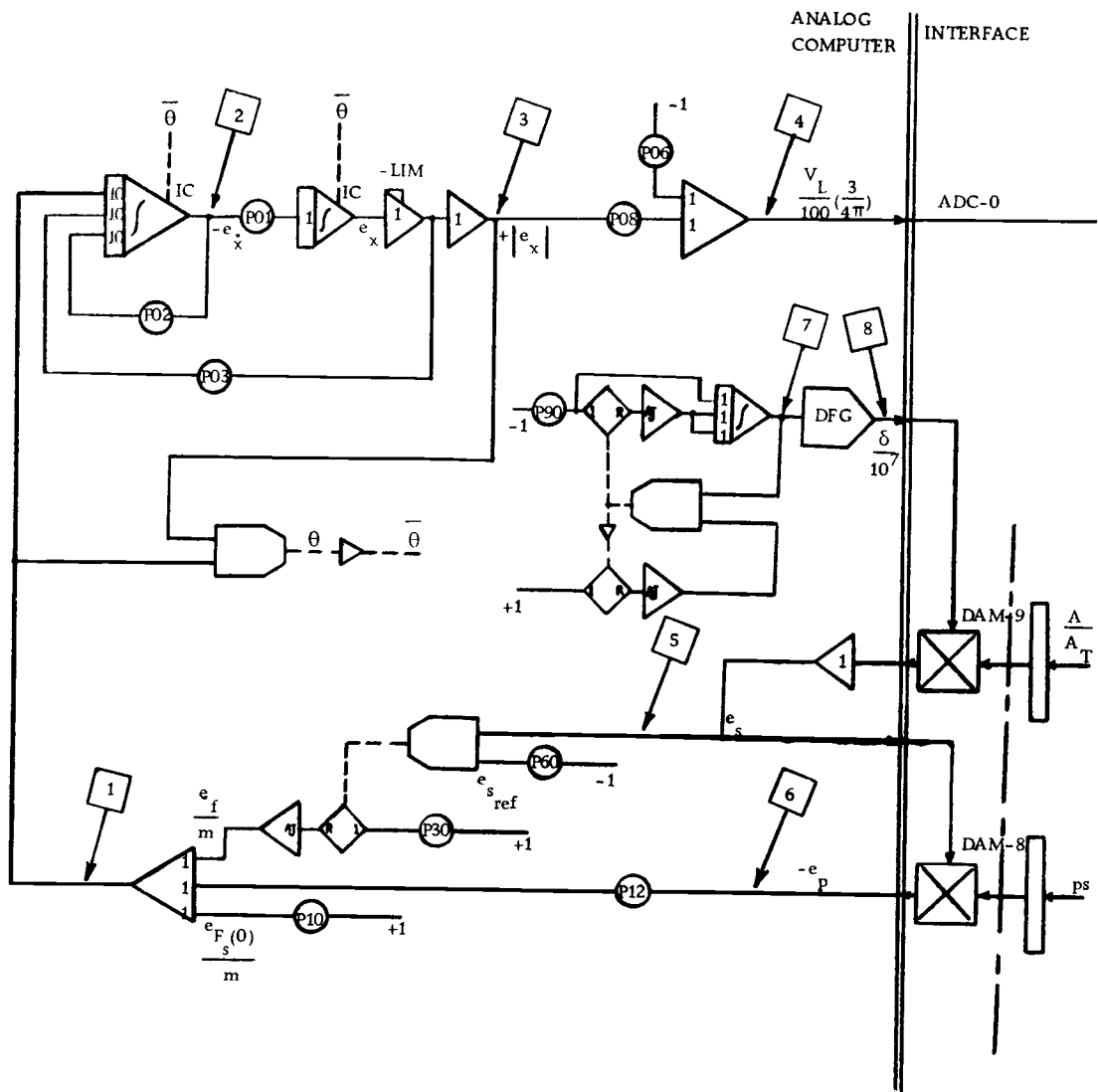


Figure B.1. Analog computer diagram of the first control system with interface shown.

Table B.1. Pot settings corresponding to the Figure B.1  
for the analog simulation of the control device I.

Pot Nos.	Parameter Relations for Pots	Pot Settings When		
		$V_T = 100$	$V_T = 60$	$V_T = 150$
PO1	Mag. Scaling $\frac{1}{s}$	.1		
PO2	$\frac{k_v}{m} (10^{-4})$	.1		
PO3	$\frac{k_s}{m} (10^{-6})$	.07		
PO6	$\frac{V_T}{(\frac{100}{100})} (\frac{3}{4\pi})$	.2388	.15	.358
PO8	$\frac{3}{4\pi}$	.2388		
P10	$e_{fs}(0)$	.01		
P12	$\frac{A_p}{m}$	.1		
P30	$\frac{e_f}{m}$	.01	.01	.015
P60	$e_{s_{ref}} = \frac{s_{ref}}{10^7}$	.57	.50	.65
P90	Freq = $\frac{1}{\eta}$	.001		

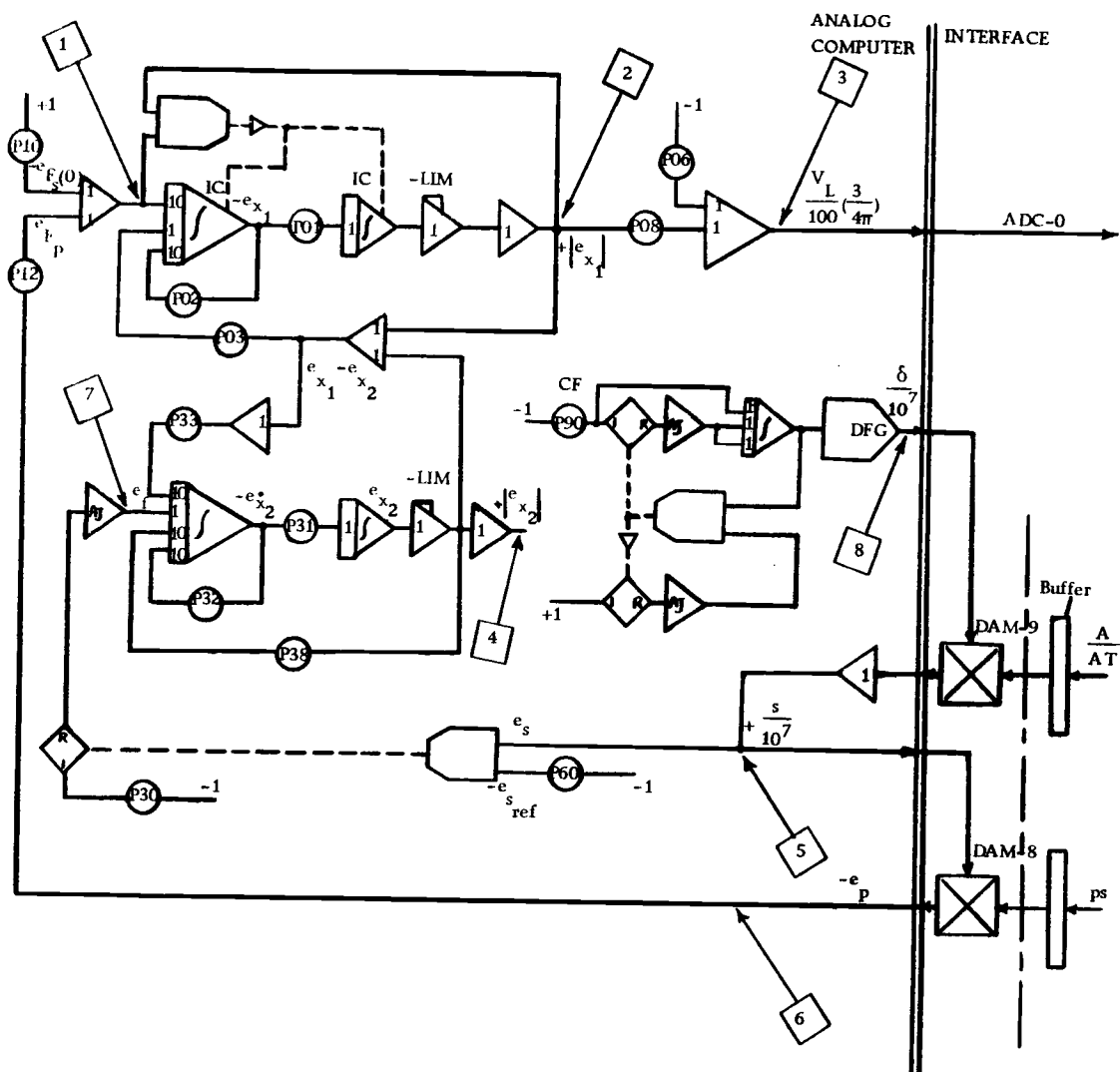


Figure B.2. Analog computer diagram of the second control system with interface shown.

Table B.2. Pot settings corresponding to the Figure B.2  
for the analog simulation of the control device II.

Pot Nos.	Parameter Relations for Pots	Pot Settings When $V_T = 100$
P01	Mag. Scaling $\frac{1}{s_1}$	.1
P02	$\frac{k_{v1}}{m_1} (10^{-4})$	.05
P03	$\frac{k_{s1}}{m_1} (10^{-5})$	.05
P06	$\frac{V_T}{100} (\frac{3}{4\pi})$	.2388
P08	$\frac{3}{4\pi}$	.2388
P10	$e_{fs}(0)$	.02
P12	$\frac{A_p}{m_1}$	.1
P30	$e_f(\frac{10}{m_2})$	.3
P31	Mag. Scaling $\frac{1}{s_2}$	.1
P32	$\frac{k_{v2}}{m_2} (10^{-4})$	.995
P33	$\frac{k_{s1}}{m_2} (10^{-6})$	.025
P38	$\frac{k_{s2}}{m_2} (10^{-6})$	.4
P60	$e_{s_{ref}} = \frac{s_{ref}}{10^7}$	.54
P90	Freq = $\frac{1}{\eta}$	.001



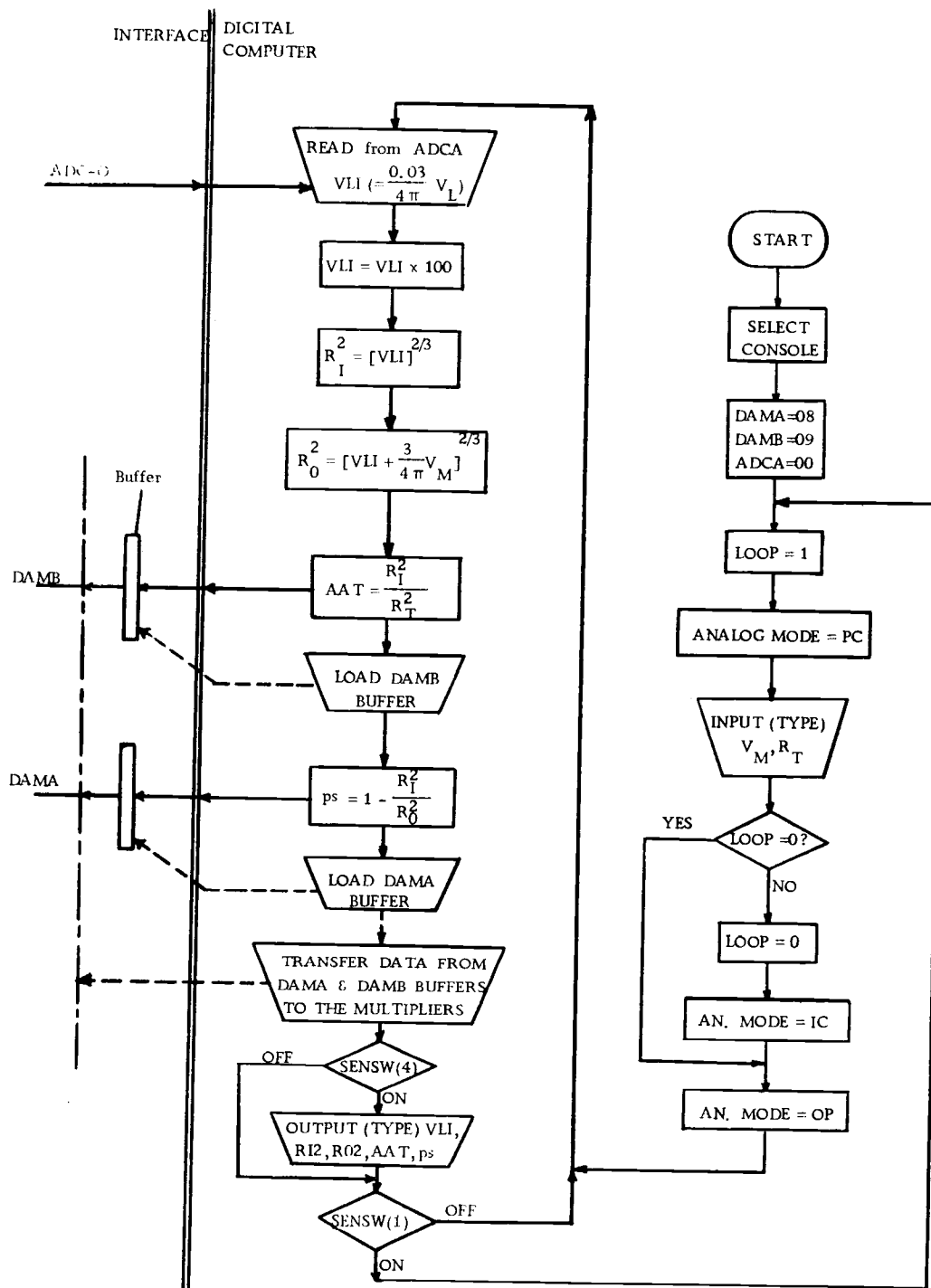


Figure B.3. Flow diagram for the digital computer portion of the system.

Table B. 3. Digital computer program using Fortran IV language.

```

CC      LEFT VENTRICLE
        INTEGER DAMA,DAMB,ADCA
        LOGICAL SENSW
        DATA PC,IC,ØP/2HPC,2HIC,2HØP/
        CALL SLCN(1,IERR)
        DAMA=Ø8
        DAMB=Ø9
        ADCA=ØØ
11      LØØP=1
        CALL SLAM (PC,IERR)
        WRITE(1,1Ø12)
1Ø12    FØRMAT(23H INPUT VM, RT; BY 2F6.5)
        READ(2,1ØØØ)VM,RT
1ØØØ    FØRMAT(2F6.5)
30      IF(LØØP.EQ.Ø)GØ TØ 4Ø
        LOOP=Ø
        CALL SLAM(IC,IERR)
        IF(IERR.EQ.1)GØ TØ 4Ø
        PAUSE 4
40      CALL SLAM(ØP,IERR)
        IF(IERR.EQ.1)GØ TØ 5Ø
        PAUSE 5
50      CALL CVADF(ADCA,VLI,IERR)
        IF(IERR.EQ.1)GØ TØ 6Ø
        PAUSE 6
60      VLI=1ØØ.Ø*VLI
        RI2=(VLI)**(Ø.6666)
        RØ2=((Ø.23878)*VM+VLI)**(Ø.6666)
        AAT=RI2/((RT)*(RT))
        CALL CVDAF(DAMB,AAT,IERR)
        IF(IERR.EQ.1)GØ TØ 7Ø
        PAUSE 7
70      PS=1.-RI2/RØ2
        CALL CVDAF(DAMA,PS,IERR)
        IF(IERR.EQ.1)GØ TØ 8Ø
        PAUSE 1Ø
80      CALL TFDA
        IF (SENSW(4)) GØ TØ 9Ø
        GØ TØ 95
90      WRITE(1,1ØØ6) VLI,RI2,RØ2,AAT,PS
1ØØ6    FØRMAT(5F9.4)
95      IF(SENSW(1))GØ TØ 11
        GØ TØ 5Ø
        END

```

## APPENDIX C

EXPERIMENTAL RESULTS FROM THE EAI 8875  
STRIP-CHART RECORDER

The results obtained from the experiments on the hybrid computer EAI 690 were recorded on an eight-channel strip-chart recorder EAI 8875. The pertinent results from the control devices I and II are shown on the following pages. All the values on the following figures except on Figure C.3, are in per unit. For the constant factors refer to pages 37 and 44.

The time on the following figures is indicated by the small markers on the top and bottom of the strip charts. The markers on the top indicate intervals of one second, and the markers on the bottom indicate intervals of ten seconds. The corresponding real time intervals are found by dividing the time intervals on the figures by 1000.

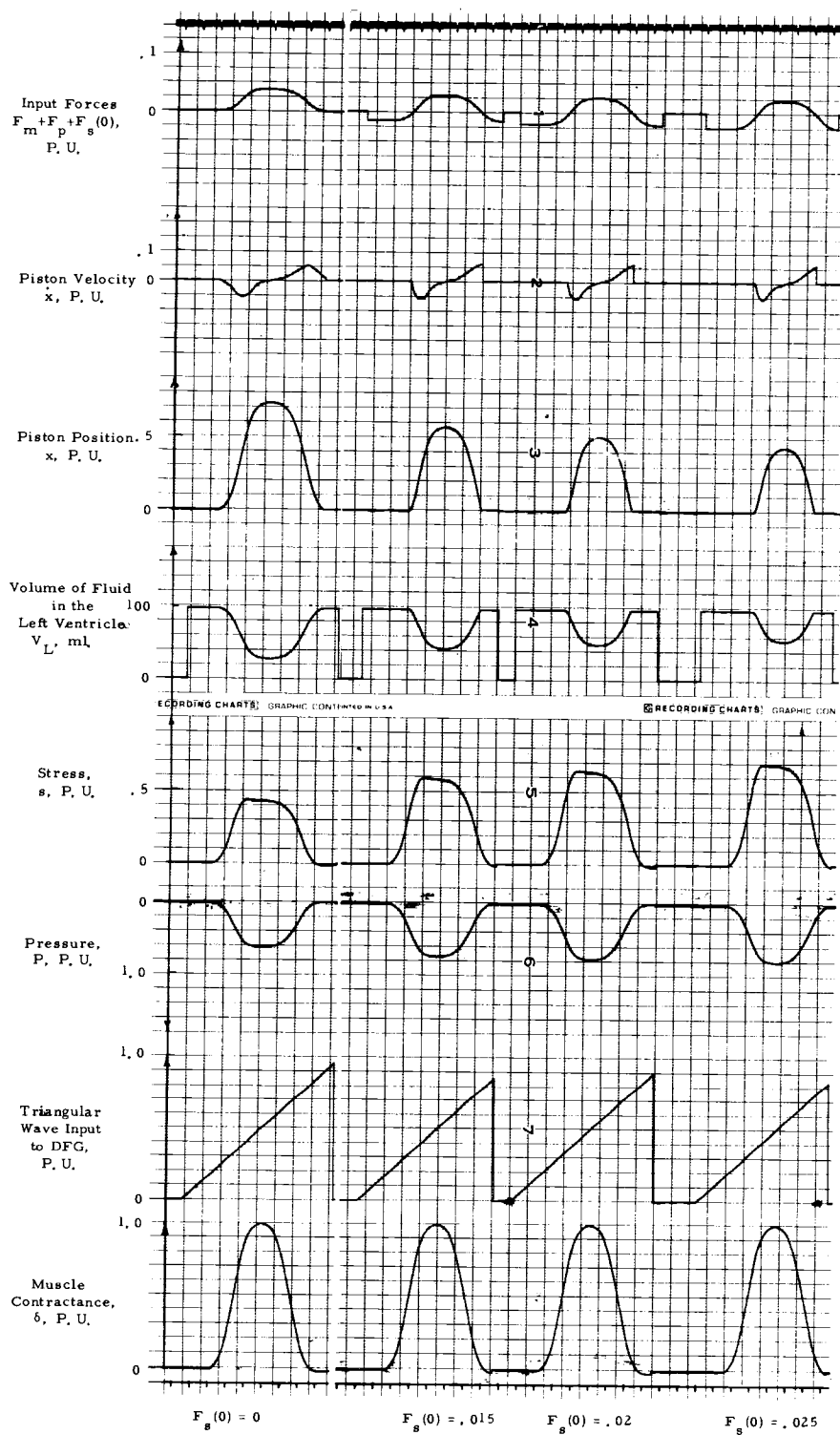


Figure C. 1. The effect of preloading of the spring  $F_s(0)$  in the control device I, without any other changes, on controlling of the stress level.

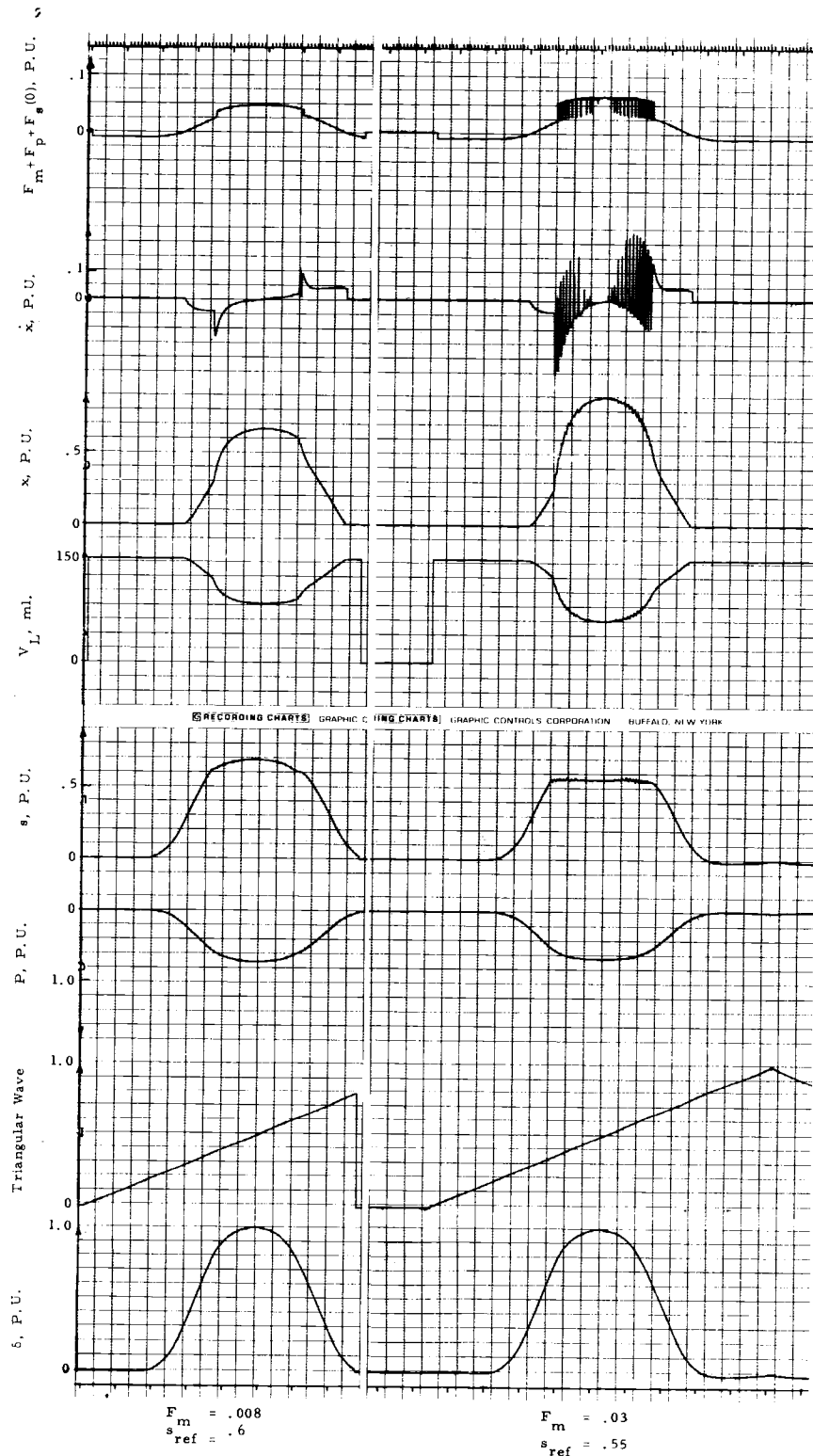


Figure C.2. The influence of the magnetic force,  $F_m$ , on control of the stress level in the left ventricle.

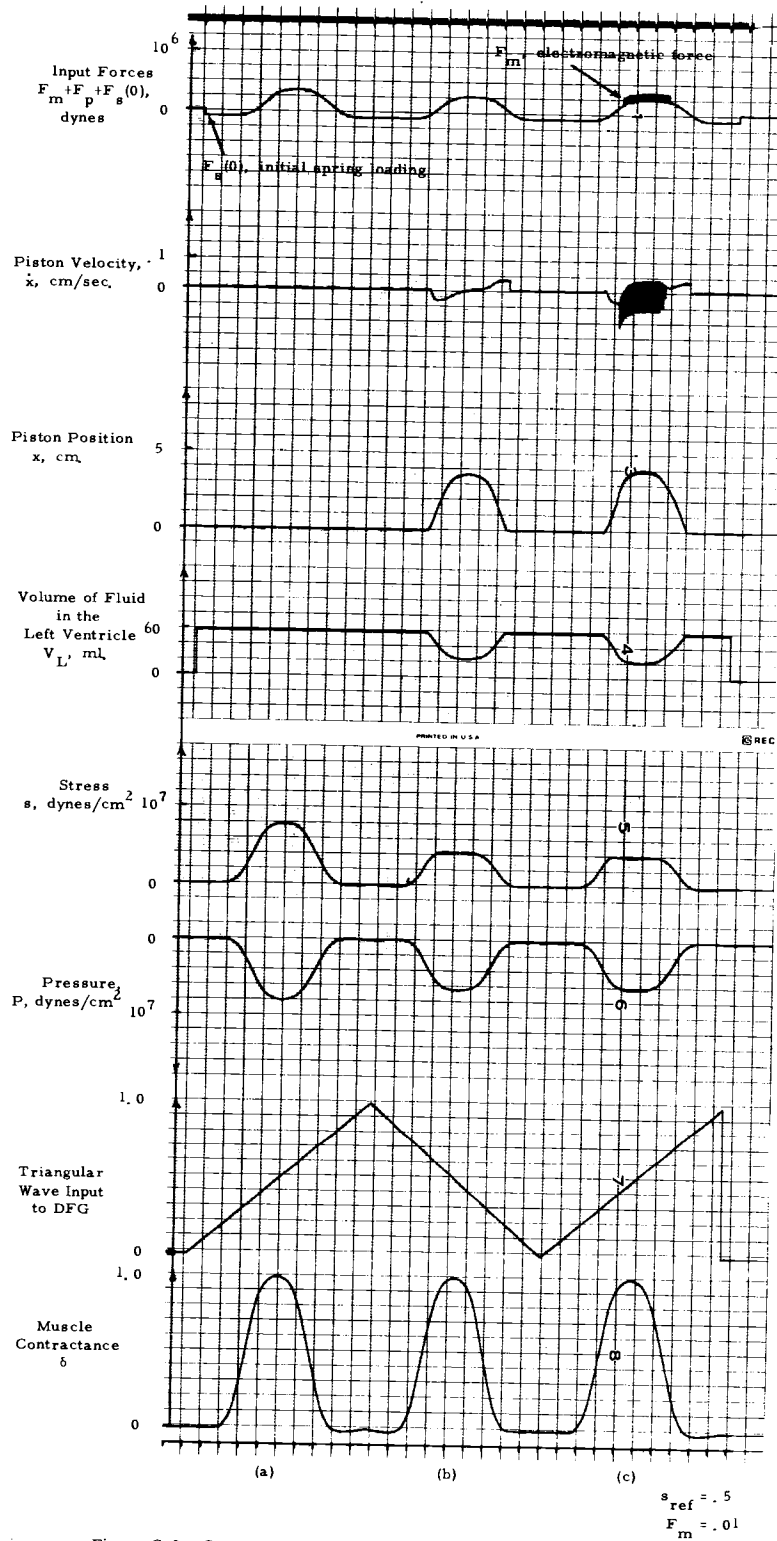


Figure C. 3. Comparison of the stress profiles in the left ventricle when (a) uncontrolled, (b) controlled without electromagnet, and (c) controlled with electromagnet, using control device I when volume,  $V_T$  is 60 ml.

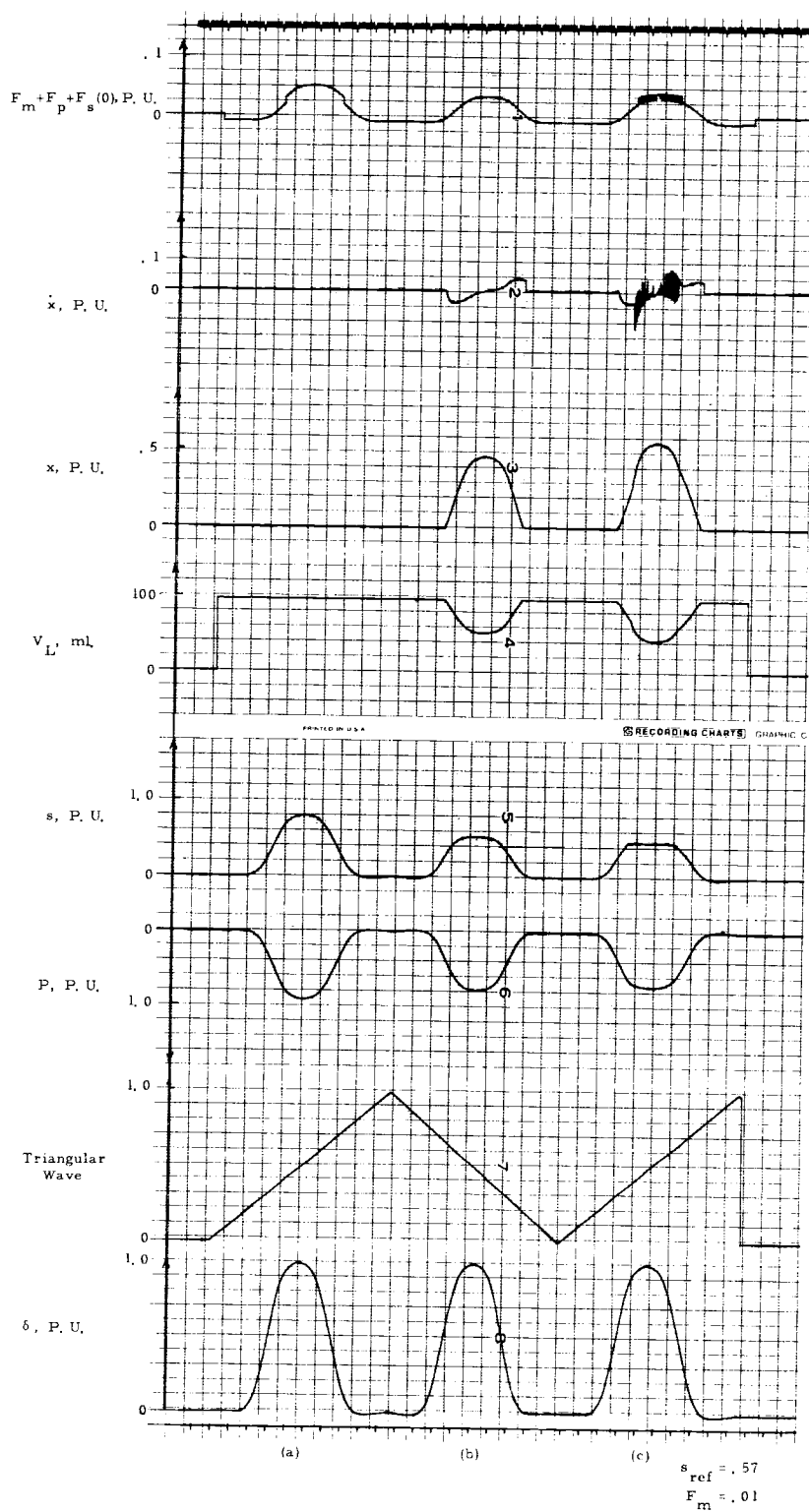


Figure C. 4. Comparison of the stress profiles in the left ventricle when (a) uncontrolled, (b) controlled without electromagnet, and (c) controlled with electromagnet, using control device I when volume,  $V_T$  is 100 ml.

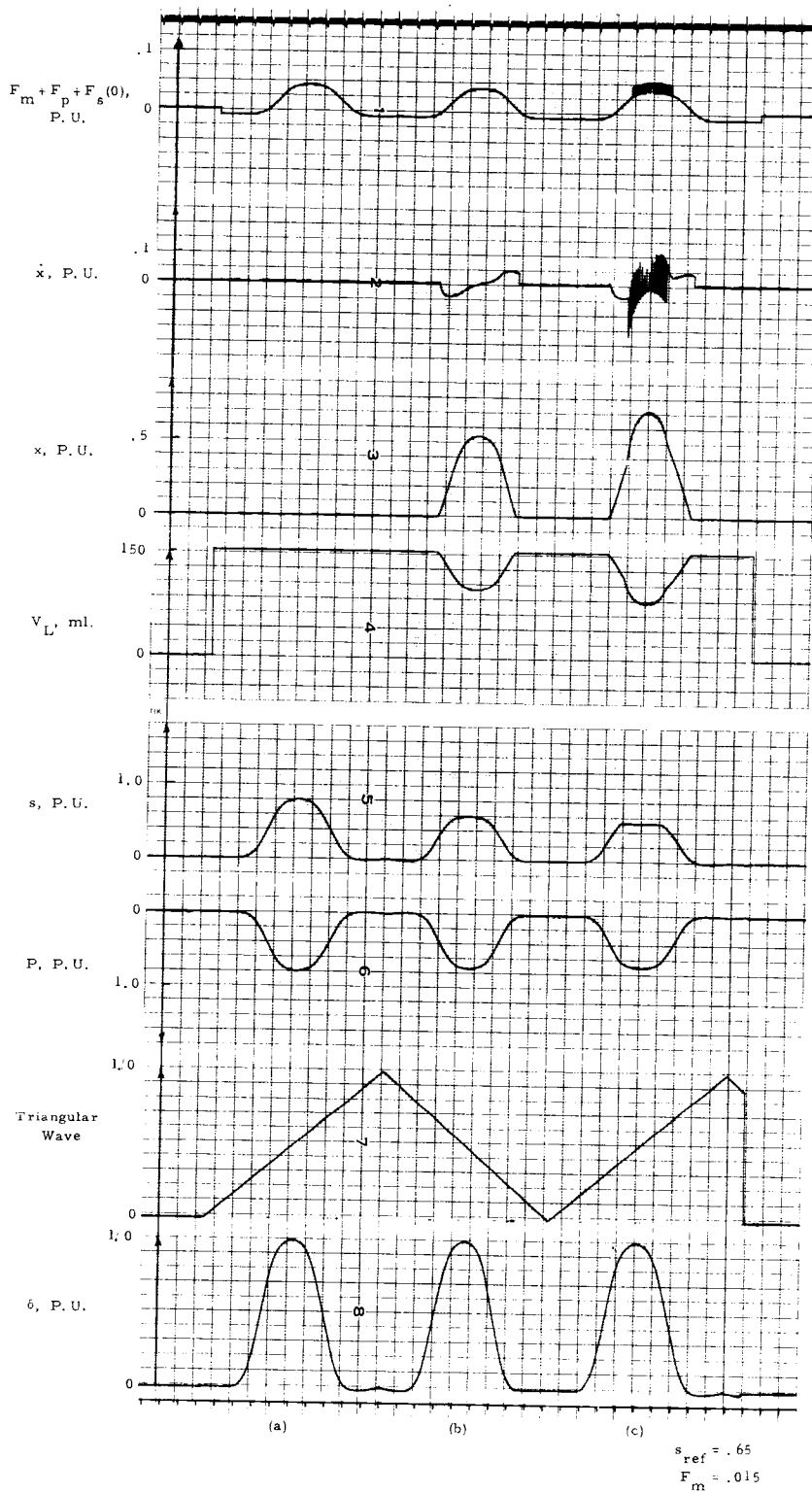


Figure C.5. Comparison of the stress profiles in the left ventricle when (a) uncontrolled, (b) controlled without electromagnet, and (c) controlled with electromagnet using control device I when volume,  $V_T$ , is 150 ml.



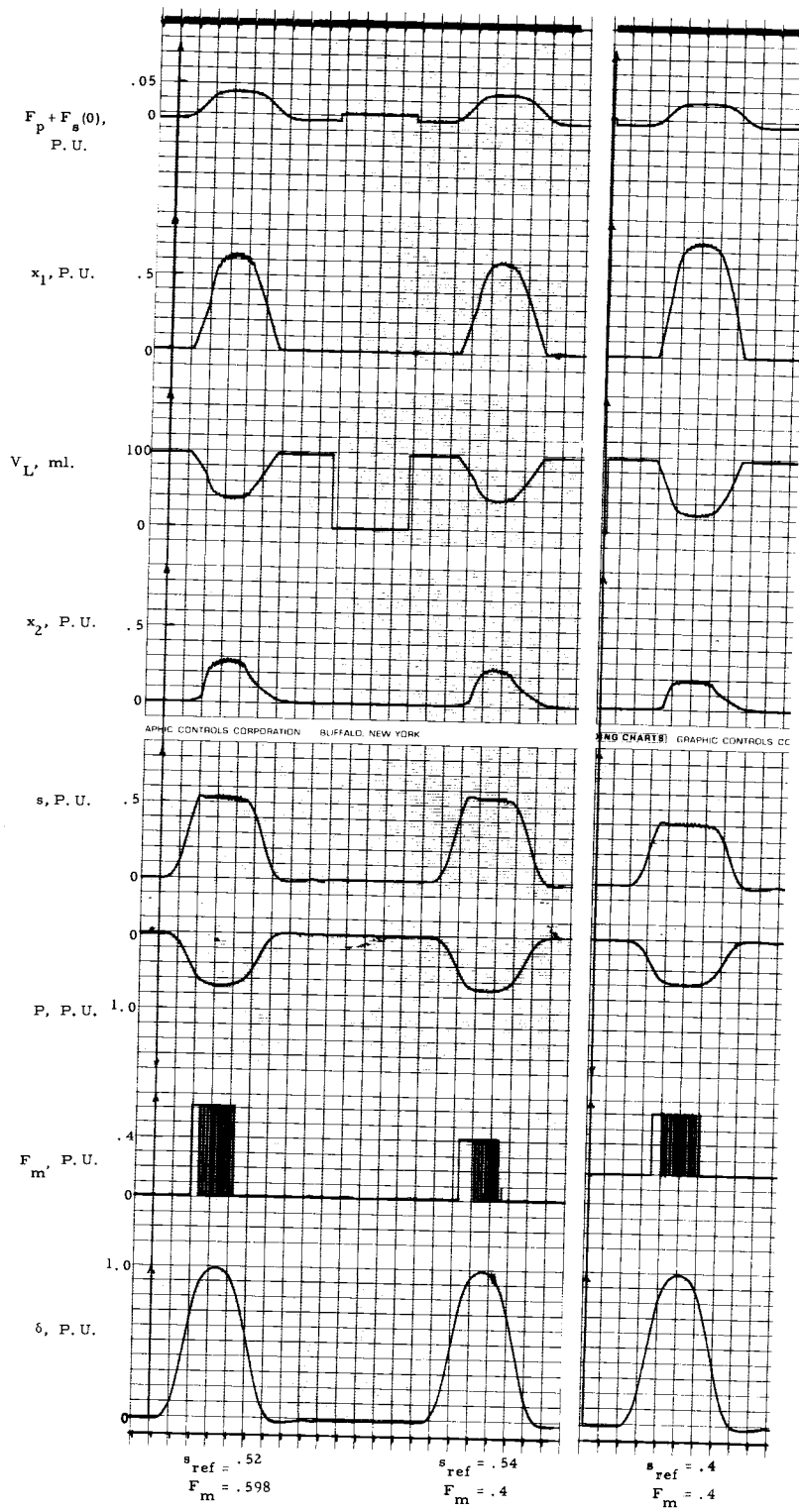


Figure C. 6. The delayed effect of the feedback electromagnetic control in the control device II.

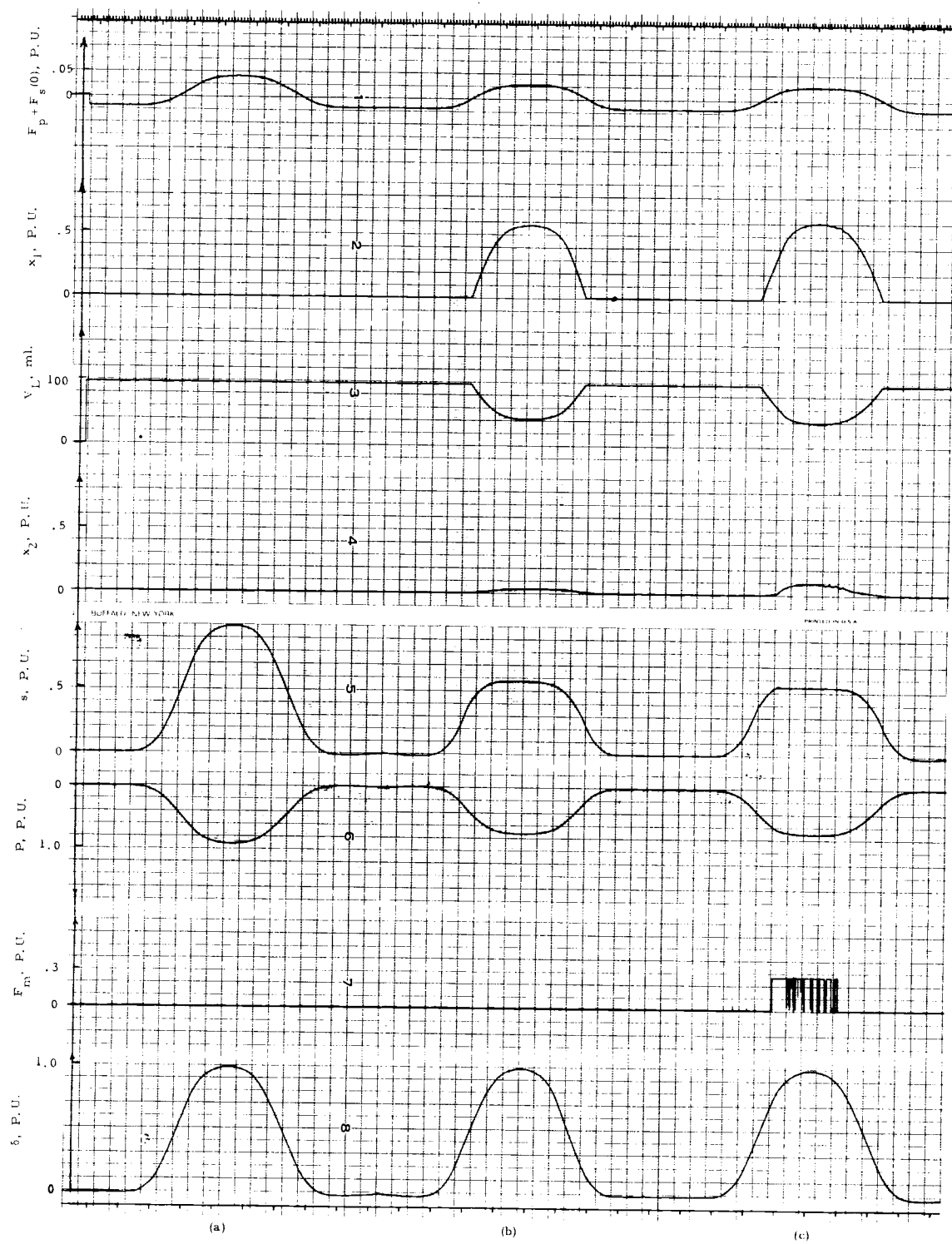


Figure C. 7. Comparison of the stress profiles in the left ventricle when (a) uncontrolled, (b) controlled without electromagnet, and (c) controlled with electromagnet using control device II.

$$s_{ref} = .54$$

$$F_m = .3$$

## APPENDIX D

PERSONAL COMMUNICATION (7)

June 30, 1967

John L. Saugen, Ph. D.  
 Oregon State University  
 School of Engineering  
 Corvallis, Oregon

Dear John:

I'm delighted to hear that you have someone that might be interested in the problem that we discussed. What I had in mind was a fairly straight forward control circuit for regulating calculated left ventricle wall stress with the objective of producing isotonic (or constantly loaded) contractions in the intact heart. In Figure I I've drawn a rough picture of the preparation. In the intact circulation blood is returned from the lungs through the left atrium and mitral valve and then is pumped by the left ventricle out the aorta. In this preparation the heart is removed from the chest and perfused by a cannula in the aorta so that the aortic valves are closed. A cannula is then inserted in the mitral valve and the left ventricle filled with saline. The entire system is shown in Figure II. A Bellofram or plunger and barrel arrangement will be used to form a closed fluid (saline) filled system. The plunger will be connected to some device to sense its position (LVDT) and force will be applied at one end to regulate the pressure within the cavity. Figure III shows the usual configuration of left ventricular pressure, volume, and wall stress in three typical states. In the first (3A) the ventricle starts to contract when active state is present, and volume is maintained constant and pressure developed. Wall stress calculated as  $PR_I^2/(R_O^2 - R_I^2)$  (where  $p$ =intracavitary pressure  $g/cm^2$ ,  $R_I$  = internal radius,  $R_O$  = external radius) for a thick wall sphere is shown in the lower panel. Panel B shows the normal course of ejection into the aorta and Panel C the desired situation where stress is maintained constant during most of the contraction. Table I has most of the maximum values and some other remarks for setting up the problem. We are currently calculating wall stress on the analog computer (TR 20) and I'll enclose a scaled diagram. Although we are still in the designing

stages for this particular application, what we are planning to do is calculate an error signal for stress on the analog and with suitable amplification drive the forcing coils on the plunger with it. The control cycle will start when wall tension reaches the level for desired control and will stop when either an arbitrary volume of fluid has been returned to the ventricle or after a preset length of time.

I hope this provides a little more detailed description of the problem. I am also enclosing a thesis by Beneken which contains a fair number of references to simulation in the cardiovascular field and the most detailed description of an analog simulation of the total cardiovascular system that I know of. If some aspect of this work or of the control system should prove interesting to someone in your group I'll be happy to help them in any way I can.

With best regards,

James W. Covell, M. D.  
Cardiology Branch  
National Heart Institute

P.S. Please return the thesis to me as soon as possible as it's the only copy I have.

Enclosures.

Table I. Maximum Values and Remarks

Pressure	400 m Hg	
Stress	400 g/cm <sup>2</sup>	
Initial Volume	100 ml	including connecting cannulae approx. 150 ml
Ejected Volume	50 ml	
Muscle Volume	150 ml	
Frequency	2 cps	basic period, significant harmonics up to 70 cps
Active State	usual duration about 300 ms - Forcing junction should not be active when active state is not present	

Fig 1

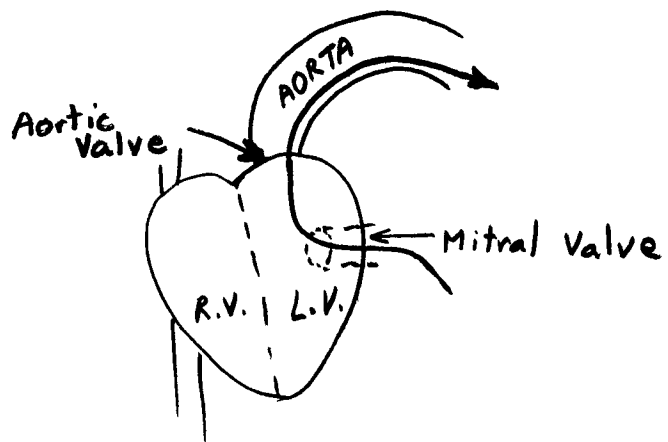


Fig 2

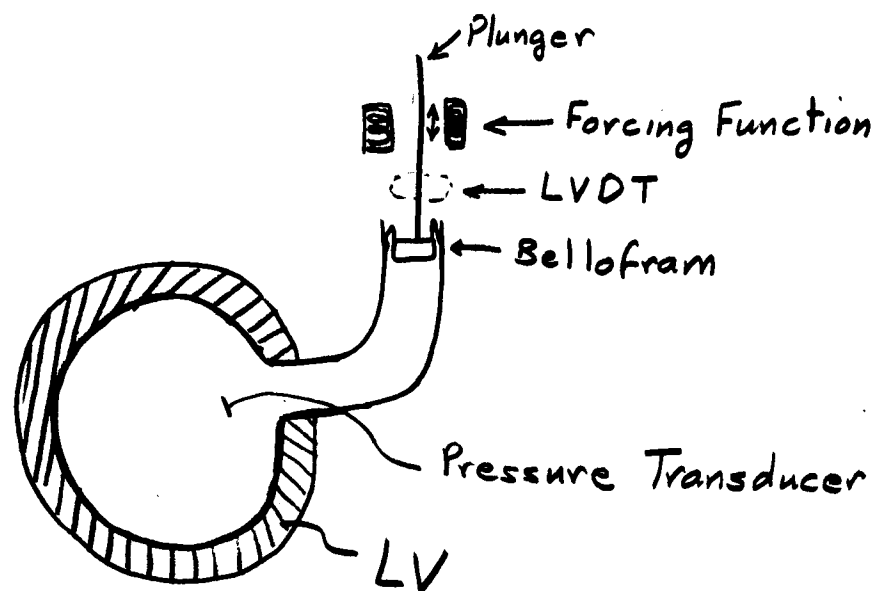


Fig 3

